National Defence
Research and Development Branch

Défense nationale
Bureau de recherche et développement

TECHNICAL MEMORANDUM 96/212
March 1996

IMPROVED BOUNDARY ELEMENT METHODS FOR PREDICTING SECTIONAL HYDRODYNAMIC COEFFICIENTS FOR STRIP THEORY SHIP MOTION PROGRAMS

Kevin A. McTaggart

Defence Research Establishment Atlantic

Centre de Recherches pour la Défense Atlantique

Canada

DEFENCE RESEARCH ESTABLISHMENT ATLANTIC

9 GROVE STREET
P.O. BOX 1012
DARTMOUTH, N.S.
B2Y 3Z7

TELEPHONE
(902) 426-3100

CENTRE DE RECHERCHES POUR LA DÉFENSE ATLANTIQUE

9 GROVE STREET
C.P. BOX 1012
DARTMOUTH, N.É.
B2Y 3Z7

National Defence
Research and Development Branch

Défense nationale
Bureau de recherche et développement

IMPROVED BOUNDARY ELEMENT METHODS FOR PREDICTING SECTIONAL HYDRODYNAMIC COEFFICIENTS FOR STRIP THEORY SHIP MOTION PROGRAMS

Kevin A. McTaggart

March 1996

Approved by C.W. Bright
Deputy Director General

Distribution Approved by C.W. Bright

Deputy Director General

TECHNICAL MEMORANDUM 96/212

Defence Research Establishment Atlantic

Centre de Recherches pour la Défense Atlantique

Canada

Abstract

This technical memorandum presents two improved boundary element methods for predicting hydrodynamic coefficients of two dimensional sections. The first method is a source distribution method, while the second is a direct method for determining velocity potential. A major objective of these improved methods is to eliminate errors due to irregular frequencies, which currently exist in the close-fit method used by the strip theory program SHIPMO. Both new methods successfully eliminate problems caused by horizontal and vertical line segments with the close-fit method. To eliminate irregular frequencies of surface-piercing sections, the source distribution method employs additional sources on a deck lid at the waterline. The introduction of a deck lid eliminates some irregular frequencies but introduces new irregular frequencies. Alternatively, a modified direct method effectively eliminates all irregular frequencies. Future strip theory implementations should incorporate this modified direct method. This technical memorandum also reviews low and high frequency limits of hydrodynamic coefficients.

Résumé

Cette note technique présente deux méthodes améliorées qui résolvent des problèmes aux frontières pour prédire les coefficients hydrodynamiques de sections bidimensionnelles. La première méthode utilise une distribution de sources tandis que la seconde est une méthode directe qui détermine le potentiel des vitesses. Un objectif très important pour améliorer ces méthodes consiste à éliminer les erreurs dues aux fréquences irrégulières, qui sont actuellement présentes dans la méthode d'ajustement que le programme SHIPMO utilise. Les deux nouvelles méthodes éliminent avec succès les problèmes que la méthode d'ajustement rencontre avec les segments de lignes horizontaux ou verticaux. Pour éliminer les fréquences irrégulières dues aux sections qui percent la surface libre la méthode par distribution de sources utilise des sources supplémentaires disposées sur un pont au niveau de la ligne de flottaison. Cette technique élimine des fréquences irrégulières mais en fait apparaître d'autres. Une autre solution consiste à utiliser une méthode directe modifiée qui élimine réellement les fréquences irrégulières. Les prochaines implémentations de la méthode de décompoition devraient comprendre cette méthode directe modifiée. Cette note technique montre également les limites basses et hautes fréquences des coefficients hydrodynamiques.

DREA TM/96/212

IMPROVED BOUNDARY ELEMENT METHODS FOR PREDICTING SECTIONAL HYDRODYNAMIC COEFFICIENTS FOR STRIP THEORY SHIP MOTION PROGRAMS

by

Kevin McTaggart

EXECUTIVE SUMMARY

Introduction

The strip theory code SHIPMO is DND's primary tool for predicting motions and loads of ships in waves. The slow development of alternative tools such as time domain codes suggests that strip theory will continue to be the primary seakeeping tool for the next several years. One of the greatest problems for strip theory computations is the presence of irregular frequencies, which can cause very large errors in hydrodynamic coefficients for surface-piercing sections. These errors adversely affect motion predictions and can severely affect load predictions. This study examines two improved boundary element methods, the source distribution method and the direct method, and their abilities for removing irregular frequencies. Prediction of hydrodynamic coefficients at the extremes of the frequency range is also examined.

Principal Results

The improved source distribution and direct methods eliminate many problems with the current close-fit method. The source distribution method with a deck lid removes some irregular frequencies but introduces new irregular frequencies. In contrast, a modified direct method effectively removes all irregular frequencies. At high frequencies, the infinite frequency limit provides an excellent approximation for velocity potential and added mass. Two dimensional methods give unrealistically high heave added mass and heave damping values for surface-piercing ship sections at low frequencies. A suitably chosen cut-off frequency appears to provide an acceptable approximation of heave added mass at lower frequencies.

Significance of Results

The modified direct method provides more reliable predictions of hydrodynamic coefficients than the close-fit method currently used in SHIPMO. Its implementation into SHIPMO will give improved ship motion and load predictions. The infinite frequency limit provides reliable values at high ship frequencies and can also be applied to impulse phenomena such as ship slamming. Better estimates of low frequency hydrodynamic coefficients will lead to better estimates of ship motions and loads at low encounter frequencies.

Future Plans

The modified direct method will replace the close-fit method in the next version of SHIPMO. The infinite frequency limit for hydrodynamic coefficients at high encounter frequency and the improved low frequency predictions will also likely be implemented.

Contents

Abstract ii

Executive Summary iii

Table of Contents v

Notation vii

1 Introduction 1

2 General Description of Problem 1

3 Source Distribution Method 4

3.1 Discretized Solution of Source Distribution Method 5

3.2 Symmetry Relations for Source Distribution Method 6

3.3 Correction of Irregular Frequencies 7

4 Direct Method 7

4.1 Improved Direct Method 9

5 Evaluation of Green Function and Its Derivatives 10

5.1 Frequency Independent Term of Green Function 11

5.2 Frequency Dependent Term of Green Function 14

6 Added Mass and Velocity Potentials at Low and High Frequency Limits 19

7 Numerical Implementation of Source Distribution and Direct Methods 20

8 Hydrodynamic Coefficients for Sample Geometries 21

8.1 Sectional Geometries for Computing Hydrodynamic Coefficients 21

8.2 Graphs of Computed Hydrodynamic Coefficients 25

8.3 Discussion of Computed Hydrodynamic Coefficients 47

9 Heave and Roll Coefficients at Low Encounter Frequency 47

10 Implementation of Improved Methods into Strip Theory Program SHIPMO 48

11 Conclusions 53

Appendix 54

A Subroutine BOUND2D for Computing Sectional Hydrodynamic Coefficients 54

References 57

Notation

$[A]$	matrix relating velocity potential to source strength
B	sectional breadth at waterline
$[B]$	matrix relating normal velocity to source strength
$[C]$	matrix relating velocity potential to vector $\{D\}$
c	wave velocity
$\{D\}$	velocity term vector for direct method
$[E]$	Green function matrix for direct method
$E_1(z_c)$	exponential integral function
$Ei(Z)$	exponential integral function
$F_{PV}(Y,Z)$	principal value function component of Green function
$G(\vec{x},\vec{x}_s)$	Green function
$\overline{G}(\vec{x},\vec{x}_s)$	frequency independent component of Green function
$\tilde{G}(\vec{x},\vec{x}_s)$	frequency dependent component of Green function
$G_0(\vec{x},\vec{x}_s)$	Green function at zero frequency limit
$G_\infty(\vec{x},\vec{x}_s)$	Green function at infinite frequency limit
g	gravitational acceleration
K_{33}	coefficient for evaluating heave added mass of ellipsoid
k	wavenumber or mode
L	ship (or ellipsoid) length
l_k	length of line segment k
l_s	source length
$\vec{n}$	normal pointing into body
$\vec{n}_{\vec{x}}$	normal pointing into body at $\vec{x}$
n_y, n_z	y and z components of normal $\vec{n}$
$n^{(k)}$	normal component for mode k
r	radius
r_{max}	maximum distance from roll origin to sectional offset points
r_1	radius from field point to image source
S_b	body surface
T	sectional draft
$\vec{V}$	velocity
V_n	normal velocity
$V_n^{(k)}$	normal velocity for mode k (time independent)
$v_n^{(k)}$	complex normal velocity for mode k (time independent)
W_j	Gaussian weighting factor for point j

Notation (continued)

$\vec{x}$	field point or source point
$\vec{x}_1, \vec{x}_2$	end points of field line segment
$\vec{x}^*$	lateral image point of $\vec{x}$
$\vec{x}_s$	source point
$\vec{x}_{s1}, \vec{x}_{s2}$	end points of source line segment
$\vec{x}_{s-j}$	quadrature point j on source line segment
Y, Z	dimensionless coordinates of field point relative to image source
y, z	horizontal and vertical coordinates
y_{max}	maximum sectional y value
z_c	complex variable $-Z + iY$
z_g	height of roll axis above waterline
α	weight term for modified direct method
α_i	angle of field point i relative to source point
α_{si}	angle of source point i relative to field point
Δ	ship (or ellipsoid) displacement
δ_{ij}	Kroenecker delta function
ζ	water surface elevation
$\vec{\eta}$	body displacement
$\vec{\eta}_k$	body displacement for mode k
θ	field line inclination angle
θ_s	source line inclination angle
λ_{ij}	damping coefficient
μ	Green function integration variable
μ_{ij}	added mass coefficient
$\vec{\xi}$	field point or source point
ρ	water density
σ	source strength
$\sigma^{(k)}$	source strength for mode k
Φ	velocity potential
ϕ	complex velocity potential (time independent)
$\phi^{(k)}$	complex velocity potential for mode k
ϕ'	revised velocity potential for low and high frequency limits
ω	oscillation frequency
$\omega_o^{(3)}$	low frequency limit for valid heave coefficients
$\omega_o^{(4)}$	lowest frequency for roll coefficient computations

1 Introduction

Strip theory ship motion programs such as SHIPMO [1, 2, 3, 4, 5, 6] are the most commonly used method for predicting ship motions and sea loads in a seaway. A key aspect of a strip theory program is the prediction of hydrodynamic coefficients of two dimensional sections. SHIPMO can predict sectional hydrodynamic coefficients using either the conformal mapping method or the Frank close-fit method [7, 8].

The conformal mapping method has various practical limitations. The geometry of an input section is customarily described by beam, draft, and area coefficient. Consequently, the method can only model sections which pierce the free surface and fall within an acceptable range of these input parameters. The limitation of using only three geometric parameters is that the conformal mapping method gives a limited approximation to the actual sectional geometry. This approximation can significantly affect roll added mass and damping predictions, which are very sensitive to sectional geometry. Another limitation of the conformal mapping method is that it does not predict sectional velocity potentials; thus, long wave approximations must be used for predicting sectional excitation forces during strip theory calculations. However, an important advantage of the conformal mapping method is its robustness.

Geometrical input for the Frank close-fit method is given in the form of sectional offsets, permitting high accuracy in input geometry. The Frank close-fit method used by SHIPMO suffers from problems as described in References 6 and 9. Input offsets for a section must have successively greater values for the vertical coordinate z; thus, the code is not able to handle a section with a flat bottom. The required spacing between vertical coordinates appears to depend partly on which computer the code is run, indicating a lack of robustness in the algorithm. A major problem of the Frank close-fit method is the presence of irregular frequencies at which results are very erratic. Irregular frequencies are common among source distribution methods for predicting hydrodynamic coefficients of a surface-piercing body. The irregular frequencies are caused by numerical solutions which satisfy prescribed boundary conditions but initiate sloshing within the body. This phenomenon occurs at the upper frequency range of interest for ship motions.

This technical memorandum examines two improved boundary element methods for predicting sectional hydrodynamic coefficients. The first method is a modified source distribution method in which a line source is placed across the waterline of a section to inhibit sloshing. Such methods have been applied previously by Bedel [10], Ohmatsu [11], and Ando [12]. The second method is a direct method as described by Sclavounos and Lee [13]. The method of Reference 13 is implemented in the DREA submarine motion code SUBMO [14, 15] without correction for irregular frequencies; the version described here includes the correction.

2 General Description of Problem

Strip theory requires a solution to the flow in the vicinity of an oscillating two dimensional section such as that shown in Figure 1. The problem of the flow around a general oscillating body is described in many references, including Kim [16], Sarpkaya and Isaacson [17], and Mei [18]. The problem is formulated in terms of an oscillatory velocity potential Φ. For the two

dimensional case, motions are limited to sway, heave, and roll. The body motions are taken as being about the center of gravity, located a distance z_g above the waterline.

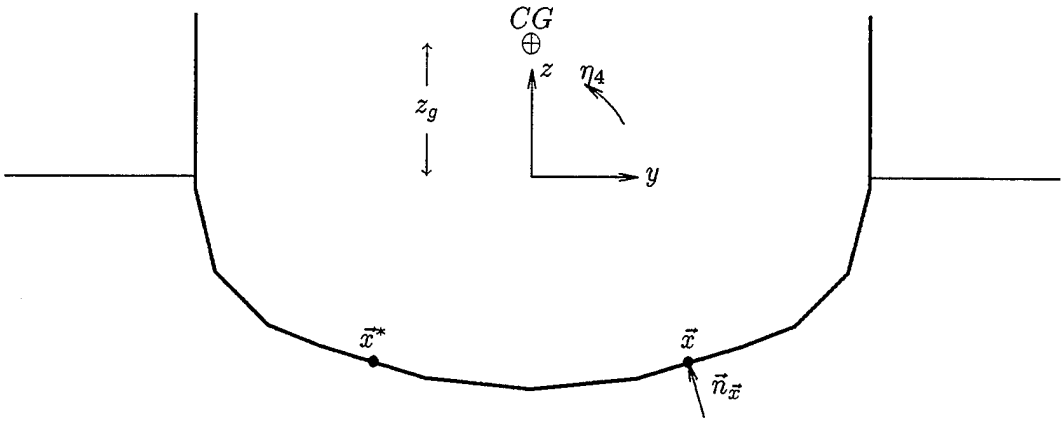

Figure 1: Two Dimensional Ship Section

The velocity potential Φ must satisfy a continuity equation and several boundary equations. Laplace's continuity equation is:

$$\nabla^2\Phi = 0 \tag{2.1}$$

Bernoulli's equation for conservation of energy must be satisfied in the fluid. Retaining only linear terms, conservation of energy imposes the following boundary condition on the free surface:

$$\frac{\partial\Phi}{\partial t} + g\,\zeta = 0 \qquad \text{at } z = 0 \tag{2.2}$$

where ζ is the elevation of waves radiated from the body. The relationship between wave elevation and the velocity potential on the surface is:

$$\frac{\partial\Phi}{\partial z} = \frac{\partial\zeta}{\partial t} \qquad \text{at } z = 0 \tag{2.3}$$

From Equations (2.2) and (2.3), the velocity potential on the free surface must satisfy:

$$\frac{\partial^2\Phi}{\partial t^2} + g\,\frac{\partial\Phi}{\partial z} = 0 \qquad \text{at } z = 0 \tag{2.4}$$

Imposing Equations (2.2), (2.3), and (2.4) at $z = 0$, the undisturbed surface, is a consequence of linearization. The following radiation condition is based on the requirement that waves generated by the oscillating body must radiate outward from the body:

$$\frac{\partial\Phi}{\partial r} + \frac{1}{c}\,\frac{\partial\Phi}{\partial t} = 0 \qquad \text{at } r = \infty \tag{2.5}$$

where r is distance from the body. The vertical water velocity must be zero at the water bottom. For deep water, this condition is:

$$\frac{\partial\Phi}{\partial z} = 0 \qquad \text{at } z = -\infty \tag{2.6}$$

The final boundary condition is that the flow into the body must be zero:

$$\frac{\partial \Phi}{\partial n} = V_n \qquad \text{on } S_b \tag{2.7}$$

where n is the normal pointing into the body and V_n is the normal velocity of the body.

For a body experiencing oscillatory motions at frequency ω, solution of the problem is greatly simplified using a time independent complex velocity potential ϕ which has the following relationship with the time dependent potential Φ:

$$\Phi(y,z,t) = \text{Real}\{\phi(y,z)\ \exp i\omega t\} \tag{2.8}$$

Thus, the complex velocity potential ϕ is merely a function of space.

In a manner similar to that used for the velocity potential, the normal velocity of the body can be expressed as a complex quantity which is independent of time:

$$\vec{V}(t) = \text{Real}\{\vec{v}\ \exp i\omega t\} \tag{2.9}$$

where $\vec{V}$ and $\vec{v}$ are the actual and time independent oscillatory velocities. For a given motion mode k, the relationship between the complex velocity $v^{(k)}$ and the complex displacement $\eta^{(k)}$ is:

$$v^{(k)} = i\,\omega\,\eta^{(k)} \tag{2.10}$$

To obtain hydrodynamic coefficients for a two dimensional section, the complex velocity potential ϕ around the body must be solved for sway, heave, and roll (denoted by modes $k = 2$, 3, and 4 respectively). From Equations (2.7), (2.8), and (2.9), the complex potentials must satisfy the following body boundary conditions:

$$\frac{\partial \phi^{(k)}}{\partial n} = v_n^{(k)} \qquad \text{on } S_b \text{ for } k = 2,3,4 \tag{2.11}$$

The complex normal velocity component $v_n^{(k)}$ for mode k is related to the body normal component $n^{(k)}$ by:

$$v_n^{(k)} = i\,\omega\,n^{(k)} \tag{2.12}$$

For motions about the center of gravity, the normals for each mode are:

$$n^{(2)} = n_y \tag{2.13}$$

$$n^{(3)} = n_z \tag{2.14}$$

$$n^{(4)} = y\,n_z + (z - z_g)\,n_y \tag{2.15}$$

Once the velocity potentials on the body are known, the added mass and damping are easily evaluated from:

$$\mu_{ij} = \frac{\rho}{\omega}\int_{S_b} \text{Imag}\left\{\phi^{(j)}\right\}\ n_i\,dS \tag{2.16}$$

$$\lambda_{ij} = \rho\int_{S_b} \text{Real}\left\{\phi^{(j)}\right\}\ n_i\,dS \tag{2.17}$$

where μ_{ij} and λ_{ij} are added mass and damping coefficients for mode i due to motion of mode j.

3 Source Distribution Method

Source distribution methods for predicting two dimensional hydrodynamic coefficients are described by many authors, including Kim [16], Sarpkaya and Isaacson [17], and Mei [18]. The Frank close-fit method [7, 8] is an example of a source distribution method.

The flow in a fluid domain can be described using a distribution of complex sources. For flow induced by a two dimensional oscillating body, the following equation can be used:

$$\phi(\vec{x}) \;=\; \frac{1}{2\pi} \int_{S_b} G(\vec{x},\vec{x}_s)\, \sigma(\vec{x}_s)\, dS \tag{3.1}$$

where $\vec{x}$ is location in the fluid domain, $\vec{x}_s$ is source location, $G(\vec{x},\vec{x}_s)$ is the Green function describing the flow at $\vec{x}$ caused by a source of unit strength at $\vec{x}_s$, and $\sigma(\vec{x}_s)$ is the strength of the source at $\vec{x}_s$.

The frequency domain Green function for a two dimensional source based on Newman [19] is:

$$\begin{aligned} G(\vec{x},\vec{x}_s) \;=\; & \ln(r) \;-\; \ln(r_1) \\ & -\, 2 \oint_0^\infty \frac{1}{\mu - 1} \exp\left[-\mu Z\right] \cos\left(\mu Y\right)\, d\mu \;+\; i\, 2\pi\, \exp(-Z)\, \cos Y \end{aligned} \tag{3.2}$$

The sign of the imaginary term in the above Green function is opposite to that given by Newman but is consistent with Kim [16] and Salvesen, Tuck, and Faltinsen [20]. The terms r and r_1 respectively denote the distance from the field point $\vec{x}$ to the source at $\vec{x}_s$ and to the image of the source above the free surface:

$$r \;=\; \sqrt{(y - y_s)^2 \;+\; (z - z_s)^2} \tag{3.3}$$

$$r_1 \;=\; \sqrt{(y - y_s)^2 \;+\; (z + z_s)^2} \tag{3.4}$$

The dimensionless coordinates Y and Z are based on wavenumber, are both positive, and are defined as follows:

$$k \;=\; \frac{\omega^2}{g} \tag{3.5}$$

$$Y \;=\; k\, |y - y_s| \tag{3.6}$$

$$Z \;=\; -k\,(z + z_s) \tag{3.7}$$

A key feature of the Green function of Equation (3.2) is that it satisfies the required conditions of Equations (2.1), (2.4), (2.5), and (2.6). The only remaining condition is the velocity boundary condition on the body (Equation (2.11)), which can be satisfied using the correct source strengths $\sigma(\vec{x})$ on the body surface. The equation for determining the source strengths that satisfy the body velocity boundary condition is:

$$-\,\frac{1}{2}\,\sigma(\vec{x}) \;+\; \frac{1}{2\pi} \int_{S_b} \frac{\partial G(\vec{x},\vec{x}_s)}{\partial n_{\vec{x}}}\, \sigma(\vec{x}_s)\, dS \;=\; v_n(\vec{x}) \tag{3.8}$$

3.1 Discretized Solution of Source Distribution Method

Equation (3.8) is normally solved by discretizing a ship section into several line segments, as shown in Figure 2. Ten line segments are usually sufficient to describe one half of a typical ship section. The source strength σ is assumed to be constant over each line segment and is such that the velocity boundary condition of Equation (2.11) is satisfied at the midpoint of each line segment. The resulting discretized form of Equation (3.8) is:

$$-\frac{1}{2}\,\sigma(\vec{x}_i) + \sum_{j=1}^{2N} \frac{1}{2\pi} \int_{S_j} \frac{\partial G(\vec{x}_i, \vec{x}_s)}{\partial n_{\vec{x}_i}}\,\sigma(\vec{x}_s)\,dS \;=\; v_n(\vec{x}_i) \tag{3.9}$$

where $2N$ is the number of segments into which the ship section has been discretized, S_j is the surface of segment j, and $\vec{x}_i$ is the midpoint of segment i. Note that the number of segments in Equation (3.9) is denoted $2N$ rather than N, which will simplify the development for symmetrical sections presented later. Once the source strengths $\sigma(\vec{x}_s)$ are known, the discretized velocity potentials can be solved using:

$$\phi(\vec{x}_i) \;=\; \sum_{j=1}^{N} \frac{1}{2\pi} \int_{S_j} G(\vec{x}_i, \vec{x}_s)\,\sigma(\vec{x}_s)\,dS \tag{3.10}$$

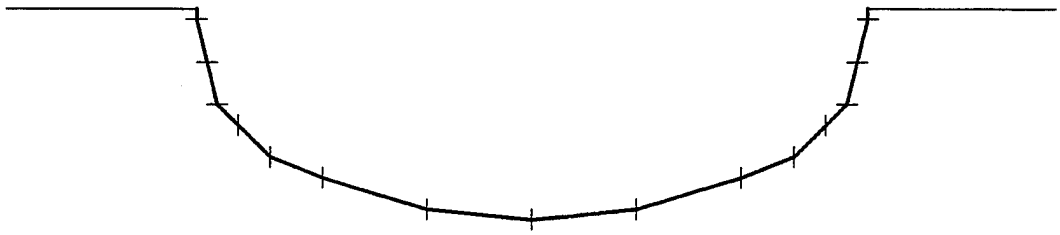

Figure 2: Discretized Ship Section for Source Distribution Method

The matrix forms of the equations relating the velocity potentials and normal velocities to the source strengths are:

$$\left\{\phi^{(k)}\right\} \;=\; [A]\,\left\{\sigma^{(k)}\right\} \tag{3.11}$$

$$\left\{v_n^{(k)}\right\} \;=\; [B]\,\left\{\sigma^{(k)}\right\} \tag{3.12}$$

From Equations (3.9) and (3.10), the matrix coefficients are:

$$A_{ij} \;=\; \frac{1}{2\pi} \int_{S_j} G(\vec{x}_i, \vec{x}_s)\,dS \tag{3.13}$$

$$B_{ij} \;=\; -\delta_{ij}\,\frac{1}{2} + \frac{1}{2\pi} \int_{S_j} \frac{\partial G(\vec{x}_i, \vec{x}_s)}{\partial n_{\vec{x}_i}}\,dS \tag{3.14}$$

where δ_{ij} is the Kroenecker delta function.

3.2 Symmetry Relations for Source Distribution Method

When running a linear ship motion program such as SHIPMO, lateral symmetry usually exists for ship sections, giving the following :

$$v_n^{(k)}(\vec{x}^*) = -\, v_n^{(k)}(\vec{x}) \qquad \text{for } k = 2,4 \tag{3.15}$$

$$v_n^{(k)}(\vec{x}^*) = v_n^{(k)}(\vec{x}) \qquad \text{for } k = 3 \tag{3.16}$$

$$\phi^{(k)}(\vec{x}^*) = -\, \phi^{(k)}(\vec{x}) \qquad \text{for } k = 2,4 \tag{3.17}$$

$$\phi^{(k)}(\vec{x}^*) = \phi^{(k)}(\vec{x}) \qquad \text{for } k = 3 \tag{3.18}$$

$$\sigma^{(k)}(\vec{x}^*) = -\, \sigma^{(k)}(\vec{x}) \qquad \text{for } k = 2,4 \tag{3.19}$$

$$\sigma^{(k)}(\vec{x}^*) = \sigma^{(k)}(\vec{x}) \qquad \text{for } k = 3 \tag{3.20}$$

where $\vec{x}^*$ is the lateral image of $\vec{x}$ defined by:

$$y^* = -\, y \tag{3.21}$$

$$z^* = z \tag{3.22}$$

Using the symmetry relations, the source strengths only need to be solved on one side of the body. If the source strengths and velocity potentials are solved for $y \geq 0$, then the coefficients for Equation (3.11) and Equation (3.12) are:

$$A_{ij}^{(k)} = \frac{1}{2\pi}\left[\int_{S_j} G(\vec{x}_i,\vec{x}_s)\, dS - \int_{S_j^*} G(\vec{x}_i,\vec{x}_s^*)\, dS\right] \qquad \text{for } k = 2,4 \tag{3.23}$$

$$A_{ij}^{(k)} = \frac{1}{2\pi}\left[\int_{S_j} G(\vec{x}_i,\vec{x}_s)\, dS + \int_{S_j^*} G(\vec{x}_i,\vec{x}_s^*)\, dS\right] \qquad \text{for } k = 3 \tag{3.24}$$

$$B_{ij}^{(k)} = -\delta_{ij}\frac{1}{2} + \frac{1}{2\pi}\left[\int_{S_j} \frac{\partial G(\vec{x}_i,\vec{x}_s)}{\partial n_{\vec{x}_i}}\, dS - \int_{S_j^*} \frac{\partial G(\vec{x}_i,\vec{x}_s^*)}{\partial n_{\vec{x}_i}}\, dS\right] \text{ for } k = 2,4 \tag{3.25}$$

$$B_{ij}^{(k)} = -\delta_{ij}\frac{1}{2} + \frac{1}{2\pi}\left[\int_{S_j} \frac{\partial G(\vec{x}_i,\vec{x}_s)}{\partial n_{\vec{x}_i}}\, dS + \int_{S_j^*} \frac{\partial G(\vec{x}_i,\vec{x}_s^*)}{\partial n_{\vec{x}_i}}\, dS\right] \text{ for } k = 3 \tag{3.26}$$

where S_j^* denotes the lateral image of S_j.

Once the velocity potentials are known for a given half-section, the added mass and damping are easily computed using the following discretized forms of Equations (2.16) and (2.17):

$$\mu_{ij} = 2\,\frac{\rho}{\omega}\sum_{k=1}^{N} l_k\, \text{Imag}\left\{\phi_k^{(j)}\right\}\, n_k^{(i)} \tag{3.27}$$

$$\lambda_{ij} = 2\,\rho\sum_{k=1}^{N} l_k\, \text{Real}\left\{\phi_k^{(j)}\right\}\, n_k^{(i)} \tag{3.28}$$

where l_k is the length of segment k.

3.3 Correction of Irregular Frequencies

A major problem with source distribution methods is the occurrence of irregular frequencies at which Equation (3.1) gives incorrect values for source strengths on an oscillating body. Irregular frequencies are caused by sloshing modes which can occur inside a surface-piercing body because the formulation (Equations 2.1 to 2.7) allows for an internal free surface. Frank [7] gives the following equation for the irregular frequencies of a heaving rectangular body:

$$\omega_j = \sqrt{\frac{j\,\pi\,g}{B}\,\coth(j\,\pi\,T/B)} \qquad \text{for } j = 1, 2, \ldots, \infty \tag{3.29}$$

For sectional computations using SHIPMO, the lowest irregular frequencies ($j = 1, 2$) typically occur at the upper portion of the frequency range of interest; thus, it is very desirable from a practical viewpoint to eliminate irregular frequency effects.

A common method for eliminating sloshing and its associated irregular frequencies is to place a deck lid across the waterline of a surface-piercing body, as described by Bedel [10], Ohmatsu [11], and Ando [12]. Figure 3 shows a ship section with a deck lid. The deck lid introduces additional line sources. An arbitrary boundary condition can be imposed on the deck lid. Generally, this boundary condition must be an odd function of y for sway and roll and an even function of y for heave. In practice, the boundary condition on the deck lid is usually specified to be that the normal velocity is zero. A variable number of sources can be used to model the deck lid. Computations by Bedel [10] and Ando [12] indicate that a small number of line segments (one or two) on the $+y$ portion of the deck lid gives the best results.

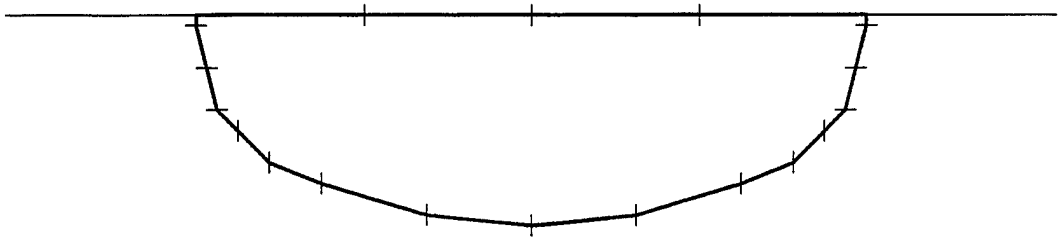

Figure 3: Discretized Ship Section with Deck Lid

4 Direct Method

The direct method is an alternative to the source distribution method, and has been described by Sclavounos and Lee [13] and Sarpkaya and Isaacson [17]. Like the source distribution method, the direct method has problems with irregular frequencies; however, Sclavounos and Lee indicate that the errors caused by irregular frequencies are less severe.

The direct method permits the direct solution of velocity potentials as follows:

$$-\frac{1}{2}\,\phi(\vec{x}) + \frac{1}{2\pi}\int_{S_b}\phi(\vec{\xi})\frac{\partial G(\vec{\xi},\vec{x})}{\partial n_{\vec{\xi}}}\,d\vec{\xi} = \frac{1}{2\pi}\int_{S_b}\frac{\partial\phi(\vec{\xi})}{\partial n_{\vec{\xi}}}\,G(\vec{\xi},\vec{x})\,d\vec{\xi} \tag{4.1}$$

where $\vec{\xi}$ is a point on the body. To permit solution of Equation (4.1), the ship section is divided into a number of discrete straight line segments, as is done for the source distribution method. The velocity potential ϕ is assumed to be constant along each segment. Equation (4.1) is satisfied at the midpoint of each segment, giving the following discretized solution of the above equation:

$$-\frac{1}{2}\,\phi(\vec{x}_i) + \sum_{j=1}^{2N}\frac{1}{2\pi}\int_{S_j}\phi(\vec{\xi})\,\frac{\partial G(\vec{\xi},\vec{x}_i)}{\partial n_{\vec{\xi}}}\,d\vec{\xi} = \sum_{j=1}^{2N}\frac{1}{2\pi}\int_{S_j}\frac{\partial\phi(\vec{\xi})}{\partial n_{\vec{\xi}}}\,G(\vec{\xi},\vec{x}_i)\,d\vec{\xi} \tag{4.2}$$

The matrix form of Equation (4.2) is:

$$[C]\,\{\phi\} = \{D\} \tag{4.3}$$

The terms of Equation (4.3) are:

$$C_{ij} = -\frac{1}{2}\,\delta_{ij} + \frac{1}{2\pi}\int_{S_j}\frac{\partial G(\vec{\xi},\vec{x}_i)}{\partial n_{\vec{\xi}}}\,d\vec{\xi} \tag{4.4}$$

$$D_i = \sum_{j=1}^{2N} v_j\,E_{ij} \tag{4.5}$$

$$E_{ij} = \frac{1}{2\pi}\int_{S_j} G(\vec{\xi},\vec{x}_i)\,d\vec{\xi} \tag{4.6}$$

For symmetrical ship sections, the symmetry conditions of Equations (3.15), (3.16), (3.17), and (3.18) apply and only the N potentials for $y \geq 0$ need to be solved. The revised matrix coefficients are:

$$C_{ij}^{(k)} = -\frac{1}{2}\,\delta_{ij} + \frac{1}{2\pi}\left[\int_{S_j}\frac{\partial G(\vec{\xi},\vec{x}_i)}{\partial n_{\vec{\xi}}}\,d\vec{\xi} - \int_{S_j^*}\frac{\partial G(\vec{\xi}^*,\vec{x}_i)}{\partial n_{\vec{\xi}}}\,d\vec{\xi}\right] \quad \text{for } k = 2,4 \tag{4.7}$$

$$C_{ij}^{(k)} = -\frac{1}{2}\,\delta_{ij} + \frac{1}{2\pi}\left[\int_{S_j}\frac{\partial G(\vec{\xi},\vec{x}_i)}{\partial n_{\vec{\xi}}}\,d\vec{\xi} + \int_{S_j^*}\frac{\partial G(\vec{\xi}^*,\vec{x}_i)}{\partial n_{\vec{\xi}}}\,d\vec{\xi}\right] \quad \text{for } k = 3 \tag{4.8}$$

$$D_i^{(k)} = \sum_{j=1}^{N} v_j^{(k)}\,E_{ij}^{(k)} \quad \text{for } k = 2,3,4 \tag{4.9}$$

$$E_{ij}^{(k)} = \frac{1}{2\pi}\left[\int_{S_j} G(\vec{\xi},\vec{x}_i)\,d\vec{\xi} - \int_{S_j^*} G(\vec{\xi}^*,\vec{x}_i)\,d\vec{\xi}^*\right] \quad \text{for } k = 2,4 \tag{4.10}$$

$$E_{ij}^{(k)} = \frac{1}{2\pi}\left[\int_{S_j} G(\vec{\xi},\vec{x}_i)\,d\vec{\xi} + \int_{S_j^*} G(\vec{\xi}^*,\vec{x}_i)\,d\vec{\xi}^*\right] \quad \text{for } k = 3 \tag{4.11}$$

4.1 Improved Direct Method

Sclavounos and Lee [13] give an improved direct method which greatly reduces irregular frequency problems of Equation (4.1). Their method combines Equation (4.1) with the following alternative direct solution:

$$-\frac{1}{2}\frac{\partial\phi(\vec{x})}{\partial n_{\vec{x}}} + \frac{1}{2\pi}\frac{\partial}{\partial n_{\vec{x}}}\int_{S_b}\phi(\vec{\xi})\frac{\partial G(\vec{\xi},\vec{x})}{\partial n_{\vec{\xi}}}\,d\vec{\xi} = \frac{1}{2\pi}\int_{S_b}\frac{\partial\phi(\vec{\xi})}{\partial n_{\vec{\xi}}}\frac{\partial G(\vec{\xi},\vec{x})}{\partial n_{\vec{x}}}\,d\vec{\xi} \quad (4.12)$$

The above equation usually gives results that are less accurate than Equation (4.1). Like Equation (4.1), Equation (4.12) has irregular frequencies; however, the two equations have different irregular frequencies.

The linear combination of Equation (4.1) and $i\alpha$ times Equation (4.12) gives the following solution for the velocity potentials:

$$-\frac{1}{2}\phi(\vec{x}) + \frac{1}{2\pi}\int_{S_b}\phi(\vec{\xi})\frac{\partial}{\partial n_{\vec{\xi}}}\left(1 + i\alpha\frac{\partial}{\partial n_{\vec{x}}}\right)G(\vec{\xi},\vec{x})\,d\vec{\xi} =$$

$$\frac{i\alpha}{2}\frac{\partial\phi(\vec{x})}{\partial n_{\vec{x}}} + \frac{1}{2\pi}\int_{S_b}\frac{\partial\phi(\vec{\xi})}{\partial n_{\vec{\xi}}}\left(1 + i\alpha\frac{\partial}{\partial n_{\vec{x}}}\right)G(\vec{\xi},\vec{x})\,d\vec{\xi} \quad (4.13)$$

where α is a constant of arbitrary value. The solution of the above equation satisfies both Equation (4.1) and Equation (4.12) if α is non-zero. An irregular frequency solution can satisfy one of Equation (4.1) or Equation (4.12), but only a real solution can satisfy both equations simultaneously; thus, the solution to Equation (4.13) typically will not have irregular frequencies if α is non-zero. Sclavounos and Lee recommend using a value of 0.2 for α, which keeps Equation (4.1) dominant but gives sufficient weight to Equation (4.12) to mitigate irregular frequencies.

The discretized form of Equation (4.13) is

$$-\frac{1}{2}\phi(\vec{x}_i) + \sum_{j=1}^{N}\frac{1}{2\pi}\int_{S_j}\phi(\vec{\xi})\frac{\partial}{\partial n_{\vec{\xi}}}\left(1 + i\alpha\frac{\partial}{\partial n_{\vec{x}_i}}\right)G(\vec{\xi},\vec{x}_i)\,d\vec{\xi} =$$

$$\frac{i\alpha}{2}\frac{\partial\phi(\vec{x}_i)}{\partial n_{\vec{x}_i}} + \sum_{j=1}^{N}\frac{1}{2\pi}\int_{S_j}\frac{\partial\phi(\vec{\xi})}{\partial n_{\vec{\xi}}}\left(1 + i\alpha\frac{\partial}{\partial n_{\vec{x}_i}}\right)G(\vec{\xi},\vec{x}_i)\,d\vec{\xi} \quad (4.14)$$

For solution using Equation (4.3), the revised matrix coefficients (neglecting symmetry) are:

$$C_{ij} = -\frac{1}{2}\delta_{ij} + \frac{1}{2\pi}\left(1 + i\alpha\frac{\partial}{\partial n_{\vec{x}_i}}\right)\int_{S_j}\frac{\partial G(\vec{\xi},\vec{x}_i)}{\partial n_{\vec{\xi}}}\,d\vec{\xi} \quad (4.15)$$

$$D_i = \frac{i\alpha}{2}v_i + \sum_{j=1}^{N}v_j\,E_{ij} \quad (4.16)$$

$$E_{ij} = \frac{1}{2\pi}\left(1 + i\alpha\frac{\partial}{\partial n_{\vec{x}_i}}\right)\int_{S_j}G(\vec{x}_i,\vec{\xi})\,d\vec{\xi} \quad (4.17)$$

For sections with lateral symmetry, solution of velocity potentials for $y \geq 0$ can be done using the following revised matrix coefficients:

$$C_{ij}^{(k)} = -\frac{1}{2}\delta_{ij} + \frac{1}{2\pi}\left(1 + i\alpha\frac{\partial}{\partial n_{\vec{x}_i}}\right)\left[\int_{S_j}\frac{\partial G(\vec{\xi},\vec{x}_i)}{\partial n_{\vec{\xi}}}\,d\vec{\xi} - \int_{S_j^*}\frac{\partial G(\vec{\xi}^*,\vec{x}_i)}{\partial n_{\vec{\xi}^*}}\,d\vec{\xi}^*\right] \text{ for } k = 2,4 \quad (4.18)$$

$$C_{ij}^{(k)} = -\frac{1}{2}\delta_{ij} + \frac{1}{2\pi}\left(1 + i\alpha\frac{\partial}{\partial n_{\vec{x}_i}}\right)\left[\int_{S_j}\frac{\partial G(\vec{\xi},\vec{x}_i)}{\partial n_{\vec{\xi}}}\,d\vec{\xi} + \int_{S_j^*}\frac{\partial G(\vec{\xi}^*,\vec{x}_i)}{\partial n_{\vec{\xi}^*}}\,d\vec{\xi}^*\right] \text{ for } k = 3 \quad (4.19)$$

$$D_i = \frac{i\alpha}{2}v_i + \sum_{j=1}^{N} v_j\,E_{ij} \text{ for } k = 2,3,4 \quad (4.20)$$

$$E_{ij} = \frac{1}{2\pi}\left(1 + i\alpha\frac{\partial}{\partial n_{\vec{x}_i}}\right)\left[\int_{S_j} G(\vec{x}_i,\vec{\xi})\,d\vec{\xi} - \int_{S_j^*} G(\vec{x}_i,\vec{\xi}^*)\,d\vec{\xi}^*\right] \text{ for } k = 2,4 \quad (4.21)$$

$$E_{ij} = \frac{1}{2\pi}\left(1 + i\alpha\frac{\partial}{\partial n_{\vec{x}_i}}\right)\left[\int_{S_j} G(\vec{x}_i,\vec{\xi})\,d\vec{\xi} + \int_{S_j^*} G(\vec{x}_i,\vec{\xi}^*)\,d\vec{\xi}^*\right] \text{ for } k = 3 \quad (4.22)$$

For a ship section with lateral symmetry and N segments on its half-section, the direct method requires solution of an $N \times N$ system of equations regardless of whether Equation (4.1) or the modified form of Equation (4.13) is used. The main burden of using the more complex equation is that additional derivatives of the Green function integrals are required. Fortunately, these additional derivatives introduce relatively little new computational effort, as discussed in the next section.

5 Evaluation of Green Function and Its Derivatives

The evaluation of the Green function of Equation (3.2) is a critical aspect of both source distribution and direct methods. Among various references discussing the two dimensional Green function (e.g. Frank [7], Kim [16], and Sarpkaya and Isaacson [17]), Newman [19] gives the most useful discussion for efficient implementation into a computer code.

The Green function of Equation (3.2) can be divided into components which are independent and dependent of frequency as follows:

$$G(\vec{x},\vec{x}_s) = \overline{G}(\vec{x},\vec{x}_s) + \tilde{G}(\vec{x},\vec{x}_s) \quad (5.1)$$

$$\overline{G}(\vec{x},\vec{x}_s) = \ln r - \ln r_1 \quad (5.2)$$

$$\tilde{G}(\vec{x},\vec{x}_s) = -2\oint_0^\infty \frac{1}{\mu - 1}\exp\left[-\mu Z\right]\cos\left(\mu Y\right)\,d\mu + i\,2\pi\,\exp(-Z)\cos Y \quad (5.3)$$

where $\overline{G}$ is the frequency independent component and $\tilde{G}$ is the frequency dependent component. The following two subsections discuss evaluation of each of the above components.

5.1 Frequency Independent Term of Green Function

The frequency independent component of the Green function is very easy to evaluate; however, the source distribution and direct methods require integration of the Green function across a source or field line. Experience has shown that the frequency independent component must be integrated accurately to obtain accurate flow solutions. Consequently, integration should be performed analytically rather than using numerical schemes such as Gaussian quadrature.

To simplify the present discussion, only the $\ln r$ term of the Green function is considered. Treatment of the $\ln r_1$ term is essentially the same.

The first integral to be considered is that from a line source with end points $\vec{x}_{s1}$ and $\vec{x}_{s2}$ to a field point x, as shown in Figure 4. The inclination of the source is:

$$\theta_s = \arctan\left(\frac{z_{s2} - z_{s1}}{y_{s2} - y_{s1}}\right) \tag{5.4}$$

The angles of the source end points relative to the field point are:

$$\alpha_{s1} = \arctan\left(\frac{z - z_{s1}}{y - y_{s1}}\right) \tag{5.5}$$

$$\alpha_{s2} = \arctan\left(\frac{z - z_{s2}}{y - y_{s2}}\right) \tag{5.6}$$

$$|\alpha_{s2} - \alpha_{s1}| \leq \pi \tag{5.7}$$

According to Comeau and Ando [21], the integral across the line source of the $\ln r$ term is:

$$\begin{aligned}
\int_{\vec{x}_{s1}}^{\vec{x}_{s2}} \ln r \, d\vec{x}_s = {} & \cos\theta_s \left\{ (y_{s1} - y_{s2}) - \frac{1}{2}(y - y_{s2}) \ln\left[(y - y_{s2})^2 + (z - z_{s2})^2\right] \right. \\
& \left. + \frac{1}{2}(y - y_{s1}) \ln\left[(y - y_{s1})^2 + (z - z_{s1})^2\right] \right\} \\
& + \sin\theta_s \left\{ (z_{s1} - z_{s2}) - \frac{1}{2}(z - z_{s2}) \ln\left[(y - y_{s2})^2 + (z - z_{s2})^2\right] \right. \\
& \left. + \frac{1}{2}(z - z_{s1}) \ln\left[(y - y_{s1})^2 + (z - z_{s1})^2\right] \right\} \\
& + (\alpha_{s2} - \alpha_{s1}) \left[(z - z_{s2})\cos\theta_s - (y - y_{s2})\sin\theta_s\right]
\end{aligned} \tag{5.8}$$

The derivatives of Equation (5.8) with respect to the field point coordinates are:

$$\int_{\vec{x}_{s1}}^{\vec{x}_{s2}} \frac{\partial \ln r}{\partial y}\, d\vec{x}_s \;=$$

$$\cos\theta_s \left\{ -\frac{1}{2}\ln\left[(y-y_{s2})^2+(z-z_{s2})^2\right] - \frac{(y-y_{s2})^2}{(y-y_{s2})^2+(z-z_{s2})^2} \right.$$

$$\left. + \frac{1}{2}\ln\left[(y-y_{s1})^2+(z-z_{s1})^2\right] + \frac{(y-y_{s1})^2}{(y-y_{s1})^2+(z-z_{s1})^2} \right\}$$

$$+ \sin\theta_s \left\{ \frac{-(z-z_{s2})(y-y_{s2})}{(y-y_{s2})^2+(z-z_{s2})^2} + \frac{(z-z_{s1})(y-y_{s1})}{(y-y_{s1})^2+(z-z_{s1})^2} \right\}$$

$$+ \left(\frac{\partial \alpha_{s2}}{\partial y} - \frac{\partial \alpha_{s1}}{\partial y} \right) \left[(z-z_{s2})\cos\theta_s - (y-y_{s2})\sin\theta_s \right] - (\alpha_{s2}-\alpha_{s1})\sin\theta_s \qquad (5.9)$$

$$\int_{\vec{x}_{s1}}^{\vec{x}_{s2}} \frac{\partial \ln r}{\partial z}\, d\vec{x}_s \;=$$

$$\cos\theta_s \left\{ \frac{-(y-y_{s2})(z-z_{s2})}{(y-y_{s2})^2+(z-z_{s2})^2} + \frac{(y-y_{s1})(z-z_{s1})}{(y-y_{s1})^2+(z-z_{s1})^2} \right\}$$

$$+ \sin\theta_s \left\{ -\frac{1}{2}\ln\left[(y-y_{s2})^2+(z-z_{s2})^2\right] - \frac{(z-z_{s2})^2}{(y-y_{s2})^2+(z-z_{s2})^2} \right.$$

$$\left. + \frac{1}{2}\ln\left[(y-y_{s1})^2+(z-z_{s1})^2\right] + \frac{(z-z_{s1})^2)}{(y-y_{s1})^2+(z-z_{s1})^2} \right\}$$

$$+ \left(\frac{\partial \alpha_{s2}}{\partial z} - \frac{\partial \alpha_{s1}}{\partial z} \right) \left[(z-z_{s2})\cos\theta_s - (y-y_{s2})\sin\theta_s \right] + (\alpha_{s2}-\alpha_{s1})\cos\theta_s \qquad (5.10)$$

The derivatives of angles α_{s1} and α_{s1} are:

$$\frac{\partial \alpha_{s1}}{\partial y} = \frac{-(z-z_{s1})}{(y-y_{s1})^2+(z-z_{s1})^2} \qquad (5.11)$$

$$\frac{\partial \alpha_{s1}}{\partial z} = \frac{y-y_{s1}}{(y-y_{s1})^2+(z-z_{s1})^2} \qquad (5.12)$$

$$\frac{\partial \alpha_{s2}}{\partial y} = \frac{-(z-z_{s2})}{(y-y_{s2})^2+(z-z_{s2})^2} \qquad (5.13)$$

$$\frac{\partial \alpha_{s2}}{\partial z} = \frac{y-y_{s2}}{(y-y_{s2})^2+(z-z_{s2})^2} \qquad (5.14)$$

The integral from a point source $\vec{x}_s$ to a field line with end points $\vec{x}_1, \vec{x}_2$ shown in Figure 5 is also required. The field line has parameters similar to the line source as follows:

$$\theta = \arctan\left(\frac{z_2-z_1}{y_2-y_1}\right) \qquad (5.15)$$

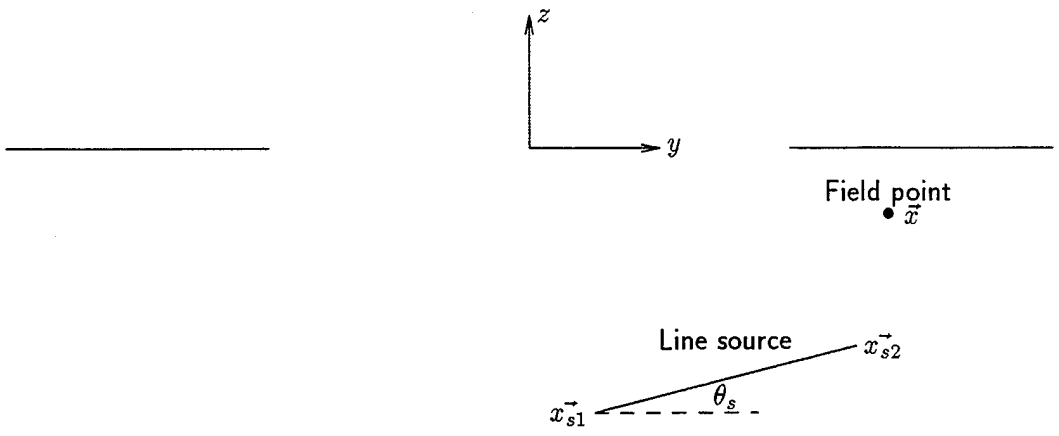

Figure 4: Line Source and Field Point

$$\alpha_1 = \arctan\left(\frac{z_s - z_1}{y_s - y_1}\right) \tag{5.16}$$

$$\alpha_2 = \arctan\left(\frac{z_s - z_2}{y_s - y_2}\right) \tag{5.17}$$

$$|\alpha_2 - \alpha_1| \leq \pi \tag{5.18}$$

The integral across the field line of $\ln r$ is essentially the same as Equation (5.8). The integral of the normal derivative of $\ln r$ along the field line is required for the direct method. When considering the orientation of the normal vector on the field line, it is assumed that field line points are numbered consecutively outward from the centerline $y = 0$ and that the normal vector to the field line points into the ship. From Comeau and Ando [21], the integral of the normal derivative on the field line is simply:

$$\int_{\vec{x}_1}^{\vec{x}_2} \frac{\partial \ln r}{\partial n_{\vec{x}}}\, d\vec{x} = \alpha_1 - \alpha_2 \qquad \text{for } y_1 \geq 0 \text{ and } y_2 \geq 0 \tag{5.19}$$

$$\int_{\vec{x}_1}^{\vec{x}_2} \frac{\partial \ln r}{\partial n_{\vec{x}}}\, d\vec{x} = -(\alpha_1 - \alpha_2) \qquad \text{for } y_1 \leq 0 \text{ and } y_2 \leq 0 \tag{5.20}$$

The derivative of Equation (5.19) with respect to the normal vector at the source point $\vec{x}_s$ is:

$$\frac{\partial}{\partial n_{\vec{x}_s}} \int_{\vec{x}_1}^{\vec{x}_2} \frac{\partial \ln r}{\partial n_{\vec{x}}}\, d\vec{x} = n_{y-\vec{x}_s}\left(\frac{\partial \alpha_1}{\partial y_s} - \frac{\partial \alpha_2}{\partial y_s}\right) + n_{z-\vec{x}_s}\left(\frac{\partial \alpha_1}{\partial z_s} - \frac{\partial \alpha_2}{\partial z_s}\right) \tag{5.21}$$

The derivative of Equation (5.20) can be similarly derived.

Special attention must be given to evaluation of the $\ln r$ integrals when the point $\vec{x}$ under consideration is the midpoint of the line segment, leading to singularities. In this situation, the

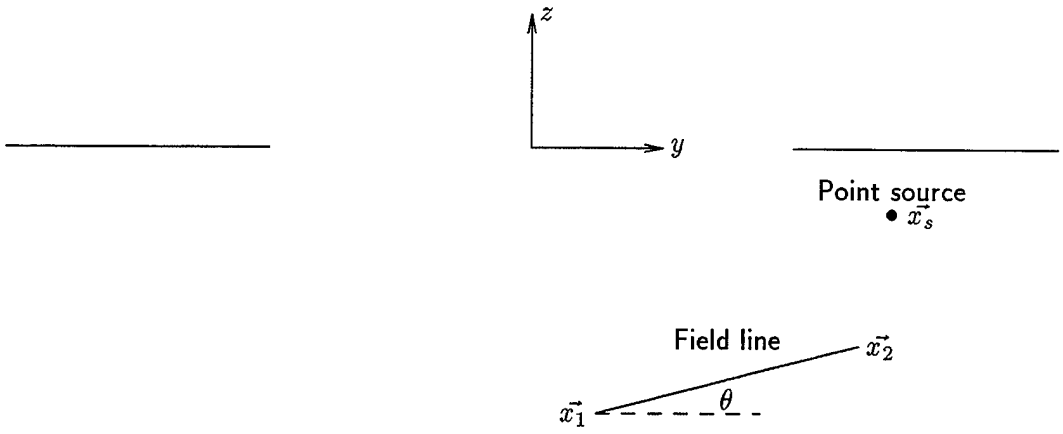

Figure 5: Field Line and Point Source

following solutions exist:

$$\int_{x_{s1}}^{x_{s2}} \ln r \, d\vec{x}_s = l_s \left[\ln\left(\frac{l_s}{2}\right) - 1 \right] \tag{5.22}$$

$$\int_{x_{s1}}^{x_{s2}} \frac{\partial \ln r}{\partial n_{\vec{x}}} \, d\vec{x}_s = 0 \tag{5.23}$$

$$\frac{\partial}{\partial n_{\vec{x}}} \int_{x_{s1}}^{x_{s2}} \frac{\partial \ln r}{\partial n_{\vec{x}_s}} \, d\vec{x}_s = \frac{4}{l_s} \tag{5.24}$$

where l_s is source length. No such singularities exist with the term $\ln r_1$, except at the waterline $z = 0$ where $\ln r$ and $\ln r_1$ cancel each other.

5.2 Frequency Dependent Term of Green Function

The frequency dependent term of the Green function is more complicated than the frequency independent term. Fortunately, its integration over a line source or field line can be accurately approximated using Gaussian quadrature with a small number of points on the line (typically less than eight).

Following Newman [19], the frequency dependent term of the Green function is evaluated as:

$$\tilde{G}(\vec{x}, \vec{x}_s) = -2 \, \text{Real} \{ F_{PV}(Y, Z) \} + i2\pi \, \exp(-Z) \, \cos(Y) \tag{5.25}$$

where $F_{PV}(Y, Z)$ is a function representing the principal value integral of Equation (5.3). Newman introduces the following complex variable z_c:

$$z_c = -Z + iY \tag{5.26}$$

The function $F_{PV}(Y,Z)$ can be re-written as:

$$F_{PV}(Y,Z) \;=\; \exp z_c \, E_1(z_c) \;+\; \pi i \, \exp z_c \tag{5.27}$$

where $E_1(z_c)$ is the exponential integral defined by:

$$E_1(z_c) \;=\; \int_{z_c}^{\infty} \frac{\exp(-t)}{t}\, dt \;, \quad |\arg(z_c)| < \pi \tag{5.28}$$

Newman gives three efficient methods for evaluating Equation (5.27) based on the ranges of Y and Z shown in Figure 6. When $|z_c|$ is small ($Y \leq 4$ and $Z \leq 8$), the following ascending series gives rapid convergence:

$$F_{PV}(Y,Z) \;=\; \exp z_c \left[-\gamma \;-\; \ln z_c \;-\; \sum_{n=1}^{\infty} \frac{(-z_c)^n}{n\, n!} \;+\; \pi i \right] \tag{5.29}$$

The above series requires approximately thirty terms to obtain convergence to six decimal places.

For large values of Y or $|z_c|$ ($Y > 4$ or $3Y > 32 - 2Z$), the $\exp z_c \, E_1(z_c)$ term of Equation (5.27) is evaluated using a continued fraction expansion:

$$\exp z_c \, E_1(z_c) \;=\; \cfrac{1}{z_c + \cfrac{1}{1 + \cfrac{1}{z_c + \cfrac{2}{1 + \cfrac{2}{z_c + \cfrac{3}{1 + \cfrac{3}{z_c + \ldots}}}}}}} \tag{5.30}$$

A disadvantage of the continued fraction expansion is that it is not possible to specify a tolerance and then to compute successive terms until that tolerance is obtained. Instead, the number of terms in the continued fraction must be decided upon before computing terms. Fortunately, excellent convergence is obtained using 40 terms for the range of Y and Z given in Figure 6.

A double series expansion is used for small values of Y and intermediate values of Z ($Y < 4$ and $3Y \leq 32 - 2Z$ and $Z > 8$):

$$F_{PV}(Y,Z) \;=\; \sum_{n=0}^{\infty} \frac{(iY)^n}{n!} \left[\sum_{m=1}^{n} \frac{(m-1)!}{Z^m} \;-\; \exp(-Z)\, Ei(Z) \right] \tag{5.31}$$

where $Ei(Z)$ is a second exponential integral from Abramowitz and Stegun [22]:

$$Ei(Z) \;=\; \int_{-\infty}^{Z} \frac{\exp t}{t}\, dt \qquad (Z > 0) \tag{5.32}$$

The exponential integral $Ei(Z)$ is easily evaluated using the following series representation from Reference 22:

$$Ei(Z) \;=\; \gamma \;+\; \ln Z \;+\; \sum_{j=0}^{\infty} \frac{Z^j}{j\, j!} \qquad (Z > 0) \tag{5.33}$$

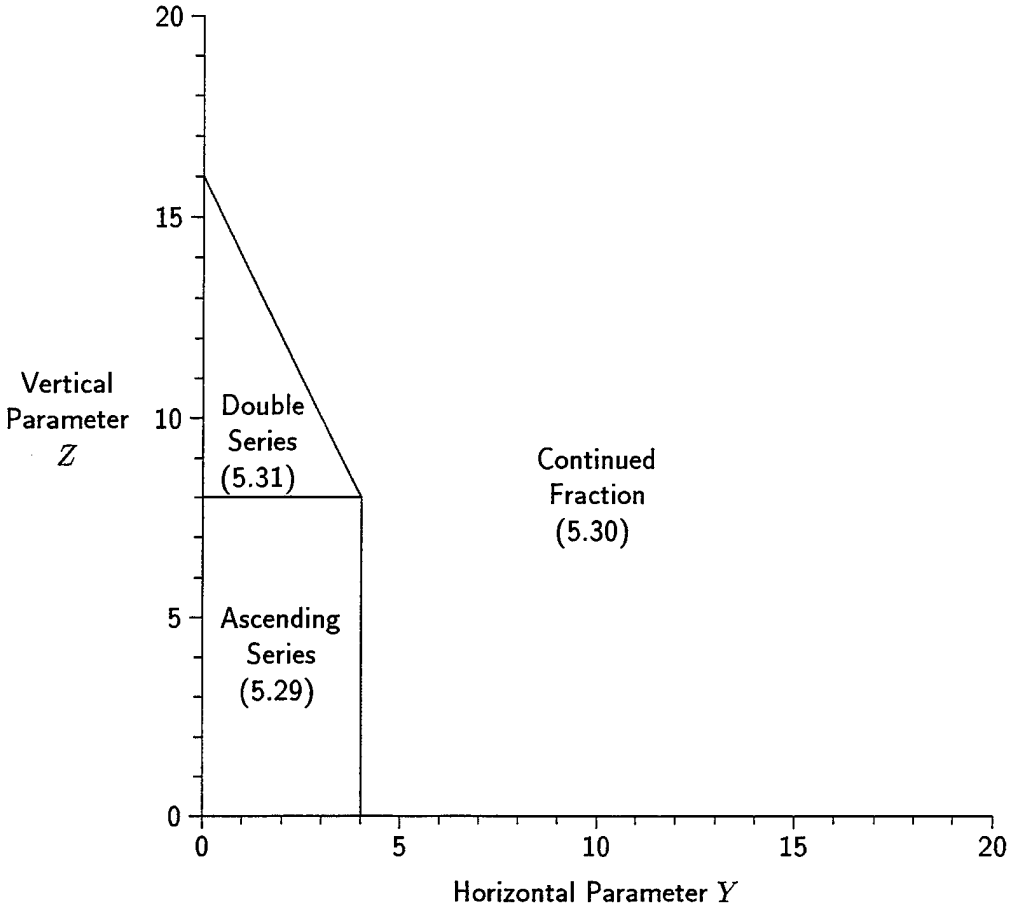

Figure 6: Ranges for Evaluation of Principal Value Integral of Green Function

Evaluation of $F_{PV}(Y,Z)$ using Equation (5.31) normally converges to 6 decimal accuracy within $n = 20$ terms.

The restriction of Equation (5.28) that $|\arg(z_c)| < \pi$ suggests that Y cannot be zero (i.e. the source and field points cannot have the same horizontal coordinates). In practice, the ascending series (Equation (5.29)) and double series (Equation (5.31)) allow $F_{PV}(Y,Z)$ to be evaluated for $Y = 0$. The only restriction on $F_{PV}(Y,Z)$ is that either Y or Z must be non-zero. Noting that Z is zero only when both the source and field point are on the waterline $z = 0$, the problematic situation of both Y and Z being zero only occurs when the source point is located on the waterline and is the same as the field point. This can occur when using a deck lid to remove irregular frequencies in the source distribution method. During computations the problem can be avoided by using Gaussian quadrature when evaluating the influence of a line source at the waterline on the flow at the line midpoint.

The derivatives of the frequency dependent part of the Green function are easily evaluated once $F_{PV}(Y,Z)$ is known. Correcting a sign error in [19], the derivatives of $F_{PV}(Y,Z)$ are:

$$\frac{\partial F_{PV}}{\partial Y} = i\,F_{PV} + \frac{i}{Z - iY} \tag{5.34}$$

$$\frac{\partial F_{PV}}{\partial Z} = -F_{PV} - \frac{1}{Z - iY} \tag{5.35}$$

Additional derivatives of $F_{PV}(Y,Z)$ are:

$$\frac{\partial^2 F_{PV}}{\partial Y^2} = -F_{PV} - \frac{1}{Z - iY} - \frac{1}{(Z - iY)^2} \tag{5.36}$$

$$\frac{\partial^2 F_{PV}}{\partial Z^2} = F_{PV} + \frac{1}{Z - iY} + \frac{1}{(Z - iY)^2} \tag{5.37}$$

$$\frac{\partial^2 F_{PV}}{\partial Y \partial Z} = -i\,F_{PV} - \frac{i}{Z - iY} - \frac{i}{(Z - iY)^2} \tag{5.38}$$

Using the above derivatives, the derivatives of the frequency dependent part of the Green function are:

$$\frac{\partial \tilde{G}(\vec{x},\vec{x}_s)}{\partial y} = -2\,k\,\mathrm{Sign}\,(y - y_s) \times \left[\mathrm{Real}\left\{iF_{PV}(Y,Z) + \frac{i}{Z - iY}\right\} + i\pi\,\exp(-Z)\,\sin Y\right] \tag{5.39}$$

$$\frac{\partial \tilde{G}(\vec{x},\vec{x}_s)}{\partial z} = 2\,k\left[\mathrm{Real}\left\{-F_{PV}(Y,Z) - \frac{1}{Z - iY}\right\} + i\pi\,\exp(-Z)\,\cos Y\right] \tag{5.40}$$

$$\frac{\partial^2 \tilde{G}(\vec{x},\vec{x}_s)}{\partial y \partial y_s} = 2\,k^2 \times \left[\mathrm{Real}\left\{-F_{PV}(Y,Z) - \frac{1}{Z - iY} - \frac{1}{(Z - iY)^2}\right\} + i\pi\,\exp(-Z)\,\cos Y\right] \tag{5.41}$$

$$\frac{\partial^2 \tilde{G}(\vec{x},\vec{x}_s)}{\partial y \partial z_s} = 2\,k^2\ \mathrm{Sign}\,(y-y_s) \times \left[\mathrm{Real}\left\{-iF_{PV}(Y,Z) - \frac{i}{Z-iY} - \frac{i}{(Z-iY)^2}\right\} - i\pi\ \exp(-Z)\ \sin Y\right] \quad (5.42)$$

$$\frac{\partial^2 \tilde{G}(\vec{x},\vec{x}_s)}{\partial z \partial y_s} = -\frac{\partial^2 \tilde{G}(\vec{x},\vec{x}_s)}{\partial y \partial z_s} \quad (5.43)$$

$$\frac{\partial^2 \tilde{G}(\vec{x},\vec{x}_s)}{\partial z \partial z_s} = \frac{\partial^2 \tilde{G}(\vec{x},\vec{x}_s)}{\partial y \partial z_s} \quad (5.44)$$

Unlike the frequency independent part of the Green function, the frequency dependent part and its derivatives can be integrated to sufficient accuracy using Gaussian quadrature. Cook [23] gives a good summary of quadrature techniques. As an example, the integral of $\tilde{G}$ from a line source can be approximated by:

$$\int_S \tilde{G}(\vec{x},\vec{x}_s)\,d\vec{x}_s = l_s \sum_{j=1}^{N_G} W_j\,\tilde{G}(\vec{x},\vec{x}_{s-j}) \quad (5.45)$$

where N_G is the number of quadrature points on the line segment, W_j is the weighting factor of point j, and $\vec{x}_{s-j}$ is the location of quadrature point j on the line source. Figure 7 shows a line source with four quadrature points. The sum of the weights W_j is equal to one. For solution of hydrodynamic coefficients using the source distribution and direct methods, between one and four quadrature points per line segment typically will give sufficient accuracy. Using an even number of quadrature points ($N_G = 2$ or 4) eliminates the problem of both Y and Z being zero when evaluating the flow induced by a deck lid source on its own midpoint.

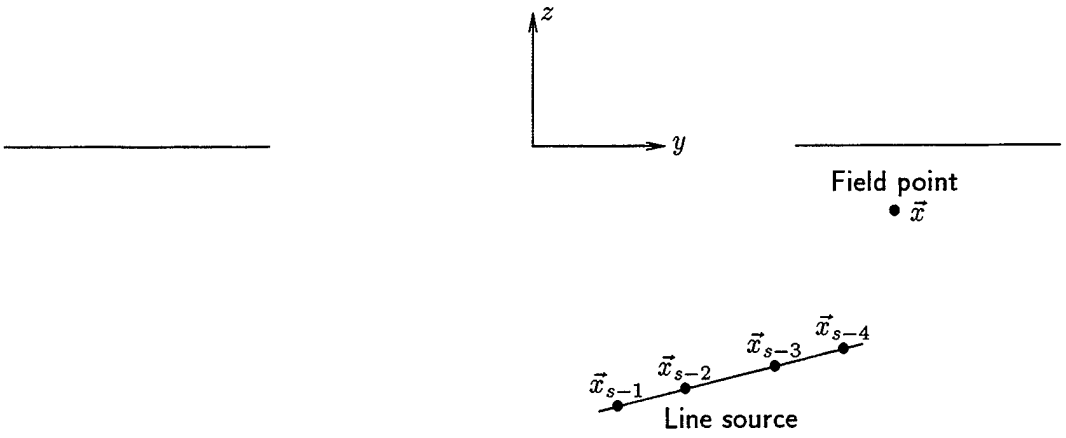

Figure 7: Gaussian Quadrature Schematic for Integration of Green Function

6 Added Mass and Velocity Potentials at Low and High Frequency Limits

The solutions for velocity potentials and hydrodynamic coefficients presented thus far do not permit solution at the low frequency limit $\omega \to 0$ or at the high frequency limit $\omega \to \infty$. A solution for $\omega = 0$ can provide a useful approximation for low frequency oscillations. A corresponding solution $\omega = \infty$ can be useful for approximating high frequency oscillations for which numerical problems can occur with the frequency dependent solutions presented previously.

To solve for added mass and velocity potential at the low and high frequency limits, the time-independent velocity potential of Equation (2.8) is replaced by:

$$\phi' = \frac{\phi}{i\,\omega} \tag{6.1}$$

The body boundary condition of Equation (2.11) simplifies to:

$$\frac{\partial \phi'^{(k)}}{\partial n} = n^{(k)} \qquad \text{on } S_b \tag{6.2}$$

The solution of ϕ' can be found using either the source distribution method or direct method described earlier.

Garrison and Berklite [24], Garrison [25], and Newman [26] discuss the solution of added mass and velocity potentials at low and high frequency limits. The surface body condition of Equation (2.4) can be expressed in terms of ϕ' as:

$$-\omega^2 \phi' + g\frac{\partial \phi'}{\partial z} = 0 \qquad \text{at } z = 0 \tag{6.3}$$

The low frequency limit of this boundary condition is:

$$\frac{\partial \phi'}{\partial z} = 0 \qquad \text{at } z = 0 \text{ for } \omega = 0 \tag{6.4}$$

The high frequency limit of the boundary condition is:

$$\phi' = 0 \qquad \text{at } z = 0 \text{ for } \omega = \infty \tag{6.5}$$

The Green function that satisfies the zero frequency boundary condition Equation (6.4) for sway motion is:

$$G_0(\vec{x}, \vec{\xi}) = \ln r + \ln r_1 \tag{6.6}$$

For heave and roll of a surface-piercing body, Newman indicates that the radiation condition of Equation (2.5) is no longer valid at zero frequency. Unfortunately, the Green function for heave and roll of a surface-piercing body at the zero frequency limit is unknown.

The Green function satisfying the infinite frequency boundary condition of Equation (6.5) is the frequency independent component of Equation (3.2):

$$G_\infty(\vec{x}, \vec{x}_s) = \ln r - \ln r_1 \tag{6.7}$$

Since the Green functions for both zero and infinite frequency are real, the potential ϕ' is real. Added mass is easily computed using the following revised form of Equation (2.16):

$$\mu_{ij} = \rho \int_{S_b} \phi'^{(j)} \, n^{(i)} \, dS \tag{6.8}$$

Approximations to the complex velocity potential ϕ at low and high frequencies can be made using Equation (6.1), with the exceptions of heave and roll for surface-piercing bodies at low frequencies.

Ursell [27] discusses the heave motion at low frequencies of elliptical sections which are half-submerged. The added mass can be approximated by:

$$\mu_{33} = \frac{\rho \, B^2}{\pi} \left[-\ln \frac{\omega^2 B}{2g} - K_{33} \right] \tag{6.9}$$

where B is the waterline breadth. Ursell gives the following equation for the coefficient K_{33}:

$$K_{33} = \ln\left(1 + \frac{2\,T}{B}\right) - 0.23 \tag{6.10}$$

where T is sectional draft. For other surface-piercing sections, one can estimate K_{33} using Equation (6.9) if added mass μ_{33} is known at a low frequency. Equation (6.9) can then be used to estimate heave added mass at other low frequencies

7 Numerical Implementation of Source Distribution and Direct Methods

Subroutines have been developed for computation of hydrodynamic coefficients using the source distribution and direct methods. The most difficult aspect of the numerical implementation was assembling the equations presented earlier in a consistent manner. Different references use different conventions for various terms, creating problems in consistent numerical implementation. For example, some references put a factor of $2/\pi$ in front of the Green function for a two dimensional source. Sign conventions for axes and normal vectors introduce additional sources of possible errors.

After obtaining the relevant equations in a consistent manner, numerical implementation of the source distribution and direct methods was relatively simple. The majority of developed source code is used by both methods; thus, the incremental effort required for having both methods available was minimal.

For integrations of Green functions across line segments, terms involving $\ln r$ and $\ln r_1$ should be integrated carefully, particularly if r and r_1 are small. The implemented code integrates terms with $\ln r$ and $\ln r_1$ exactly for all cases. For the frequency dependent part of the Green function, Gaussian quadrature using four quadrature points on the line segment gives sufficient accuracy.

8 Hydrodynamic Coefficients for Sample Geometries

This section gives hydrodynamic coefficients for various sample geometries. The sample computations provide useful information regarding irregular frequencies, differences between the various methods, and behaviour at lower and upper frequency limits.

8.1 Sectional Geometries for Computing Hydrodynamic Coefficients

Eight different sectional geometries are used for testing the source distribution and direct methods. The geometries shown in Figures 8 to 15 represent a broad range of sections for which hydrodynamic coefficients are required. Table 1 gives the offset coordinates for the sections. The first three geometries are representative of the bow, midship, and transom sections of the frigate example in the SHIPMO6 manual [6]. The fourth section is a barge designed to test the robustness of the algorithms for horizontal and vertical line segments for which the close-fit method can cause problems. The fifth section is a submarine cross-section which includes the submarine sail (validation of the SUBMO2 code in Reference 28 indicates that SUBMO2 overpredicts roll excitation moment on a submarine with a sail). The last three sections are circles at various depths of submergence.

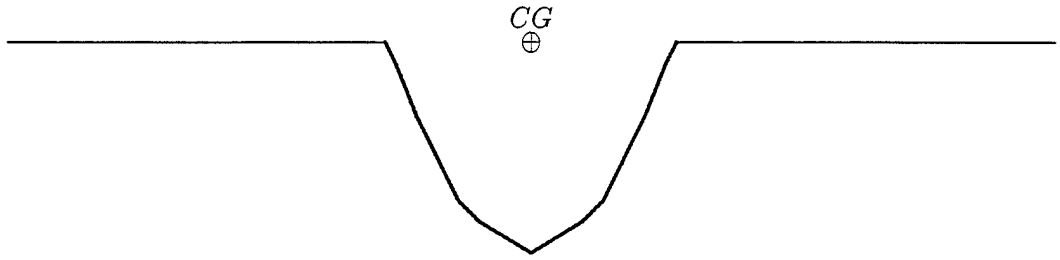

Figure 8: Bow Section of Frigate

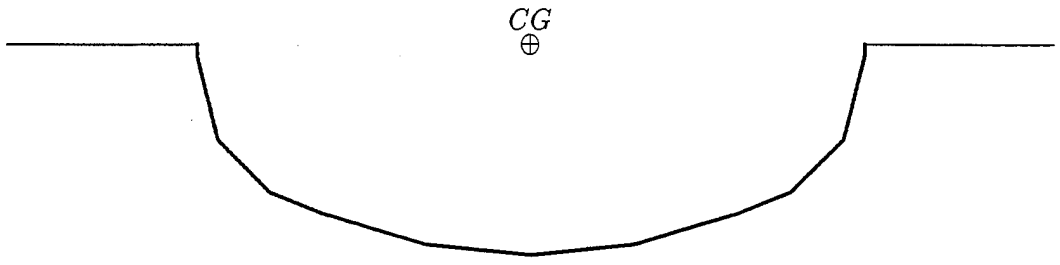

Figure 9: Midship Section of Frigate

Figure 10: Transom Section of Frigate

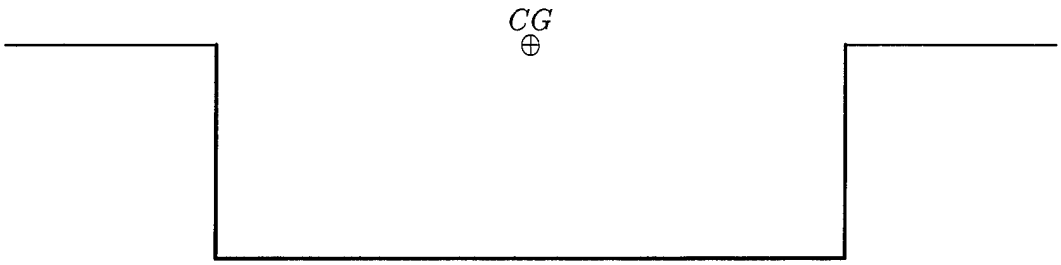

Figure 11: Barge Section

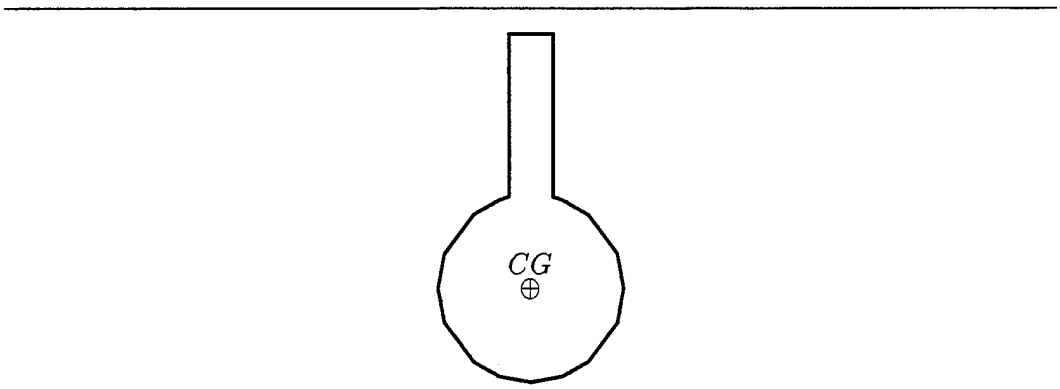

Figure 12: Submarine Section with Sail

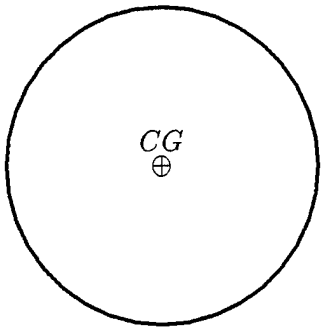

Figure 13: Deep Circle Section

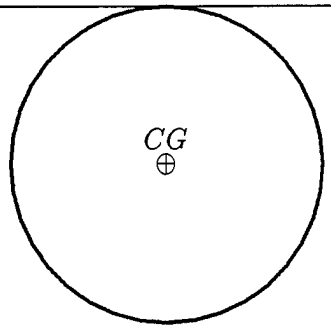

Figure 14: Shallow Circle Section

Table 1: Sectional Offsets for Hydrodynamic Coefficients

Bow

y 0 1 1.4 1.8 2.2 2.6 2.8

z -4 -3.4 -3 -2.2 -1.4 -0.4 0

Midship

y 0 2 4 5 5.6 6 6.2 6.4 6.4

z -4 -3.8 -3.2 -2.8 -2.2 -1.8 -1 -0.2 0

Transom

y 0 1.4 1.8 2.2 2.4 2.8 2.9 3

z -1 -0.9 -0.85 -0.8 -0.6 -0.4 -0.2 0

Barge

y 0 2 4 6 6 6 6 6

z -4 -4 -4 -4 -3 -2 -1 0

Submarine with sail

y 0 0.06 0.11 0.165 0.1775 0.165 0.11 0.06 0.0416 0.0416 0.0416 0.0416 0.0416 0.03 0.015 0

z -0.708 -0.697 -0.669 -0.595 -0.53 -0.465 -0.391 -0.363 -0.357 -0.33 -0.23 -0.13 -0.048 -0.048 -0.048 -0.048l

Deep circle

y 0.000 1.042 2.052 3.000 3.857 4.596 5.196 5.638 5.909 6.000 5.909 5.638 5.196 4.596 3.857 3.000 2.052 1.042 0.000

z -18.000 -17.909 -17.638 -17.196 -16.596 -15.857 -15.000 -14.052 -13.042 -12.000 -10.958 -9.948 -9.000 -8.143 -7.404 -6.804 -6.362 -6.091 -6.000

Shallow circle

y 0.000 1.042 2.052 3.000 3.857 4.596 5.196 5.638 5.909 6.000 5.909 5.638 5.196 4.596 3.857 3.000 2.052 1.042 0.000

z -12.000 -11.909 -11.638 -11.196 -10.596 -9.857 -9.000 -8.052 -7.042 -6.000 -4.958 -3.948 -3.000 -2.143 -1.404 -0.804 -0.362 -0.091 0.000

Surface-piercing circle

y 0.000 1.042 2.052 3.000 3.857 4.596 5.196 5.638 5.909 6.000 5.909 5.638 5.196 4.596 3.857 3.317

z -11.000 -10.909 -10.638 -10.196 -9.596 -8.857 -8.000 -7.052 -6.042 -5.000 -3.958 -2.948 -2.000 -1.143 -0.404 0.000

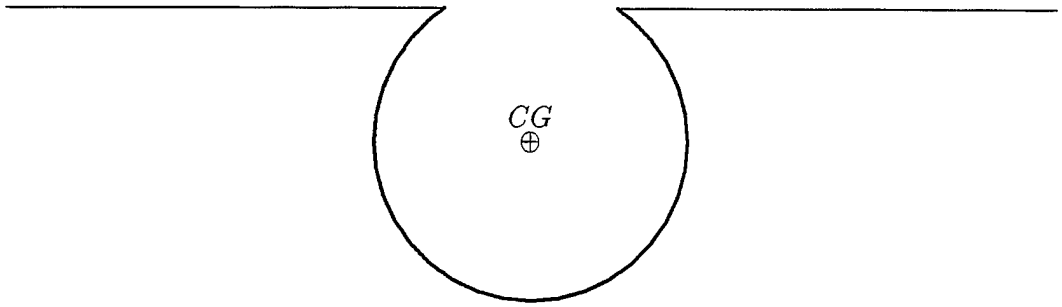

Figure 15: Surface-Piercing Circle Section

8.2 Graphs of Computed Hydrodynamic Coefficients

Figures 16 to 57 give added mass and damping coefficients for the various sections. Water density ρ is not factored into the plotted values. Computational methods include the direct method ($\alpha = 0$), modified direct method ($\alpha = 0.2$), source distribution method (no lid), and source distribution method with lid. The source distribution method with lid is used only for surface-piercing sections, with the lid represented by two line segments.

A $\otimes$ symbol at the lower and upper frequency limits gives zero and infinite frequency added mass where applicable. Each page shows added mass and damping plotted to the same scale for a given section and mode. The damping is divided by frequency so that the added mass and damping figures for a given section and mode give the relative magnitudes of the added mass and damping forces. Roll added mass and damping are zero for the circular sections; thus, no plots are shown.

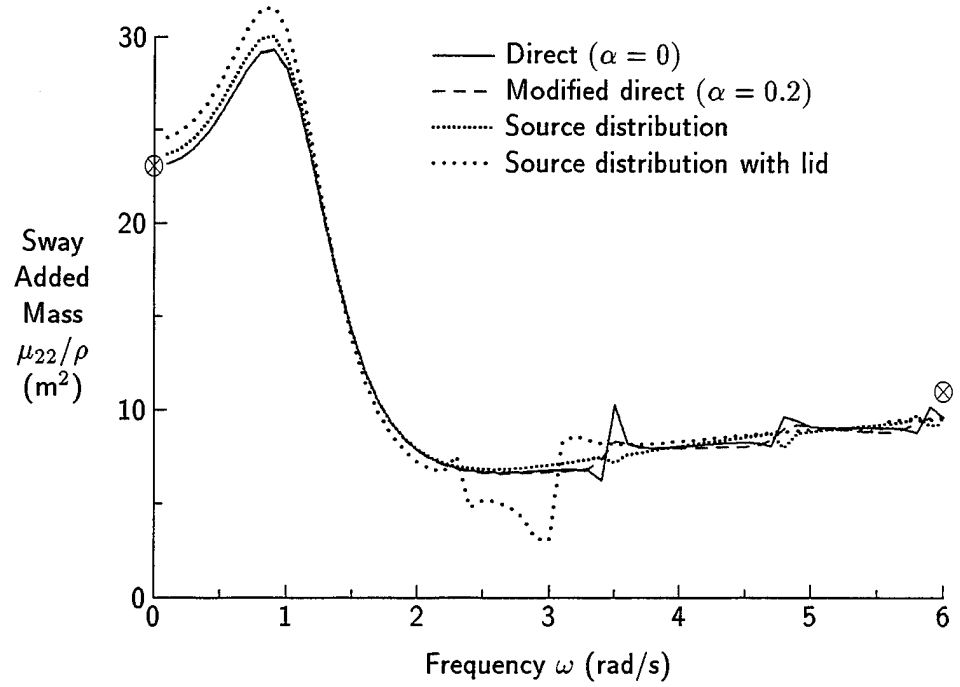

Figure 16: Sway Added Mass for Bow Section

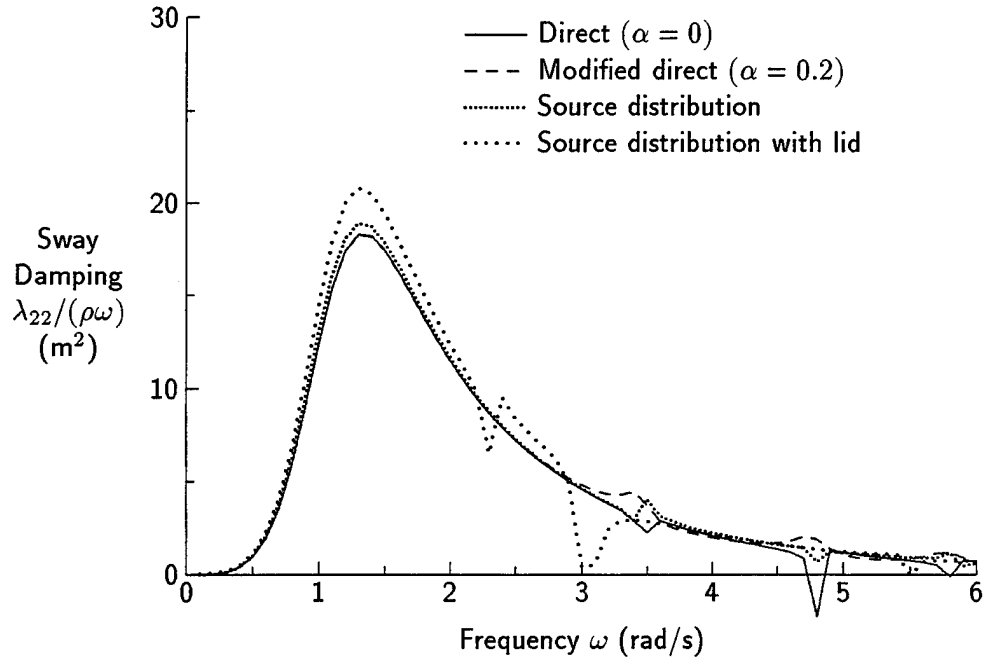

Figure 17: Sway Damping for Bow Section

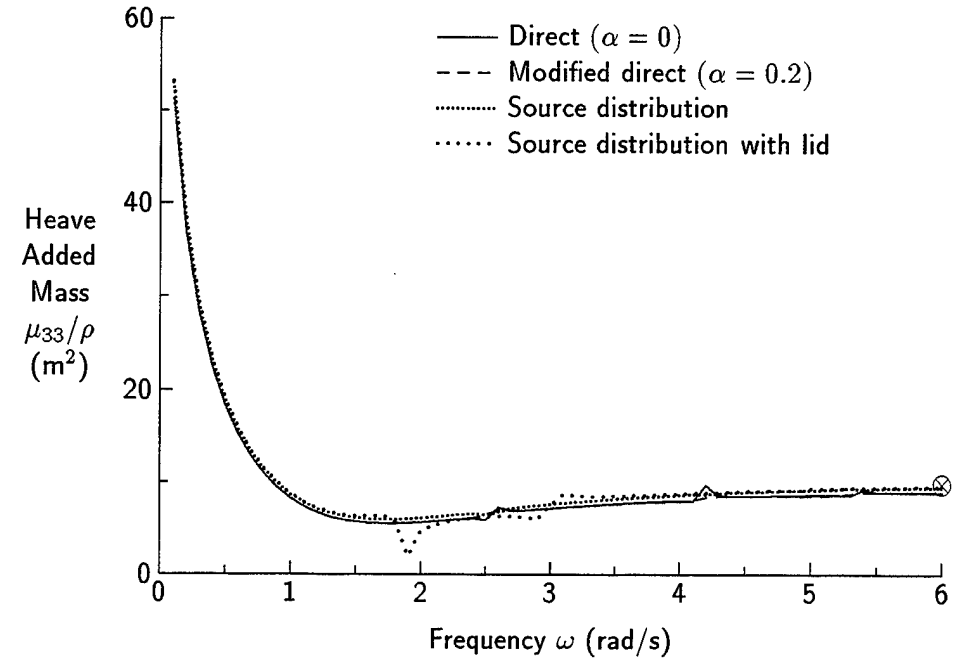

Figure 18: Heave Added Mass for Bow Section

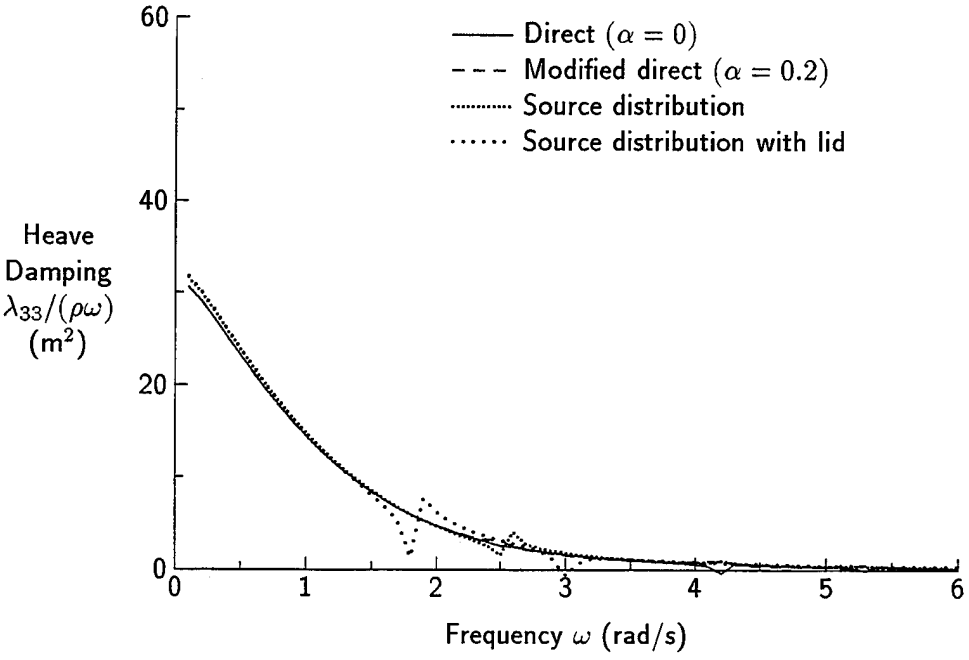

Figure 19: Heave Damping for Bow Section

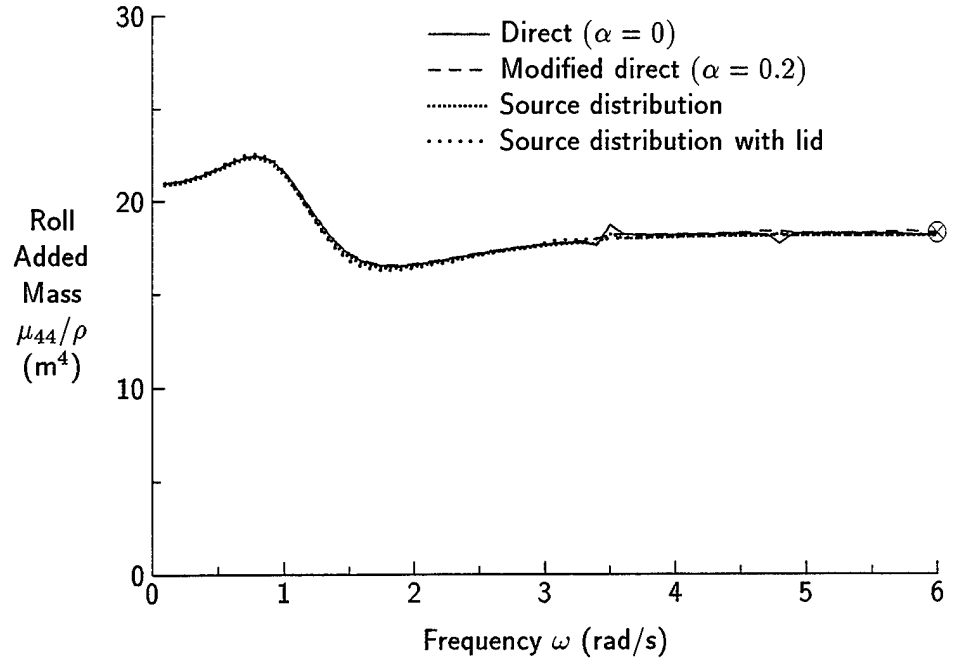

Figure 20: Roll Added Mass for Bow Section

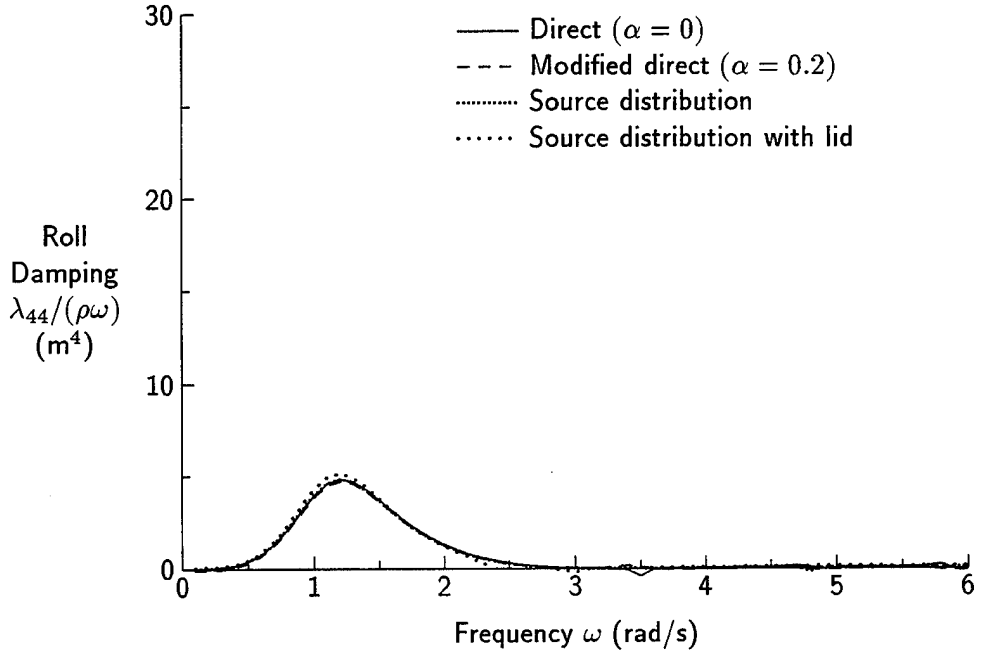

Figure 21: Roll Damping for Bow Section

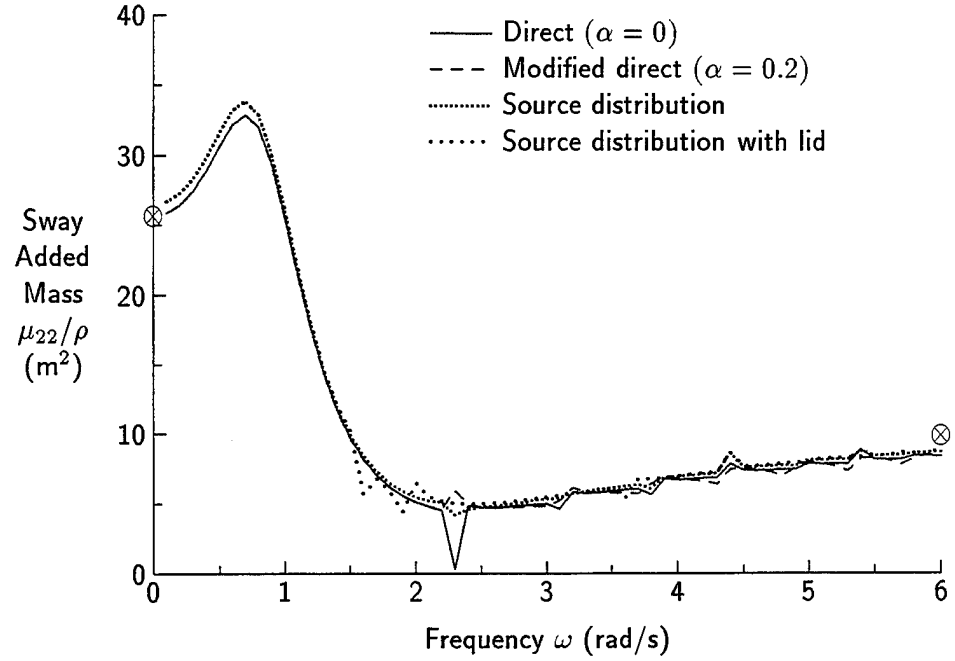

Figure 22: Sway Added Mass for Midship Section

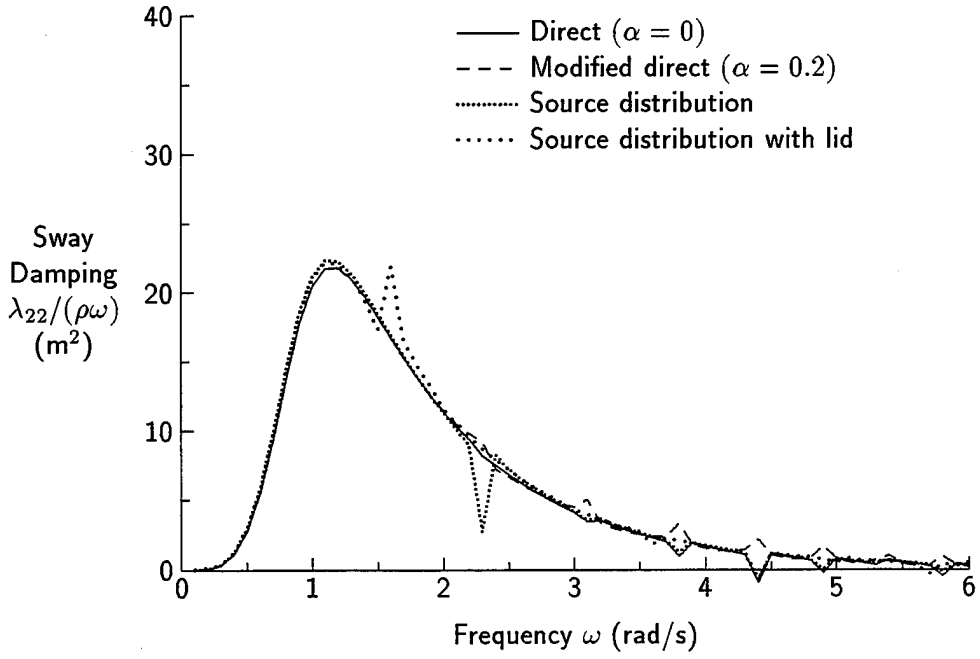

Figure 23: Sway Damping for Midship Section

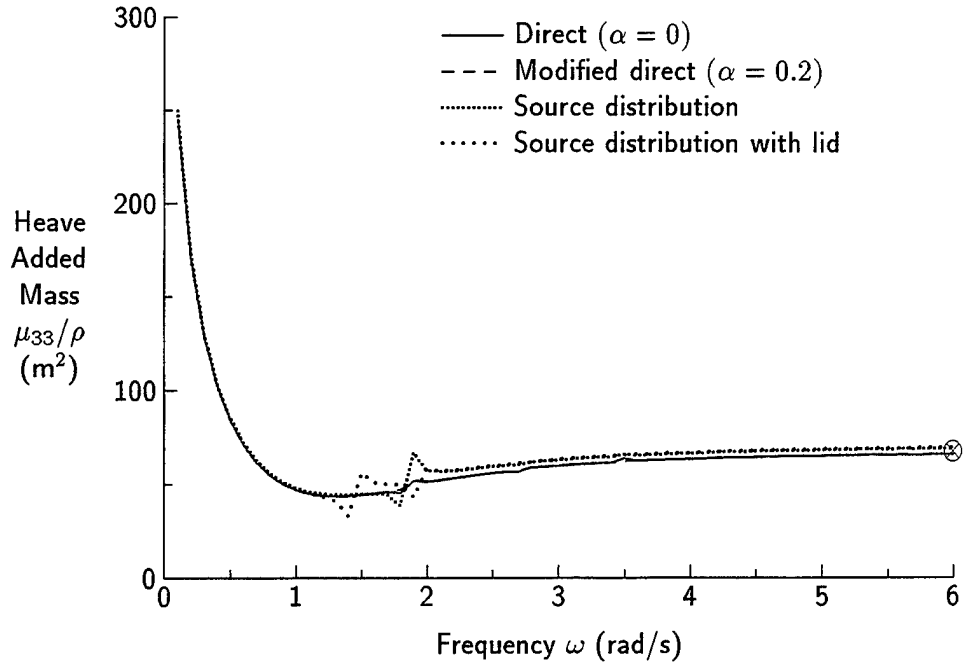

Figure 24: Heave Added Mass for Midship Section

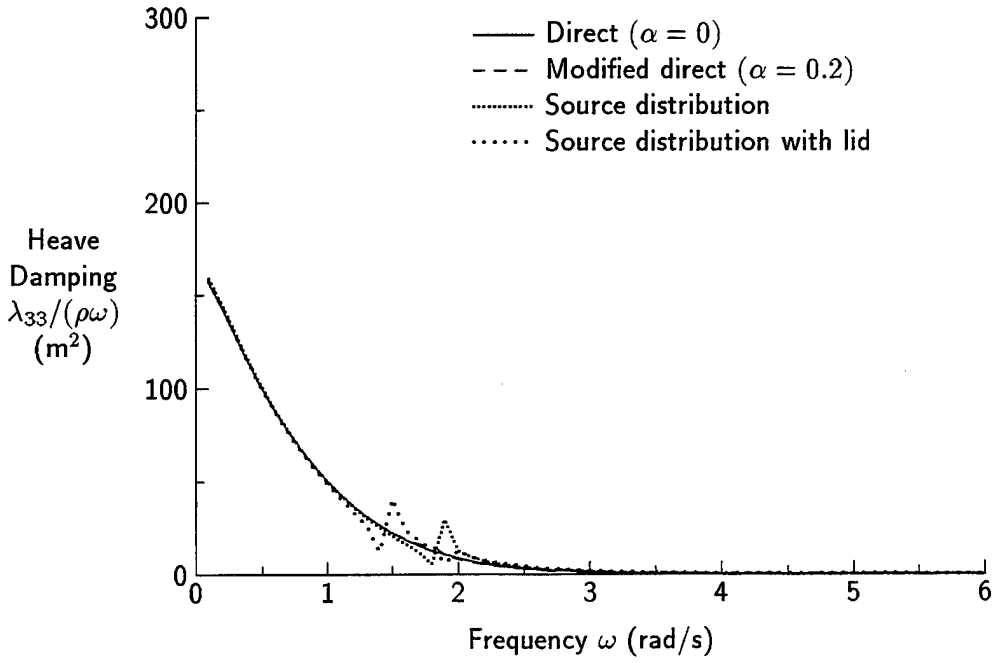

Figure 25: Heave Damping for Midship Section

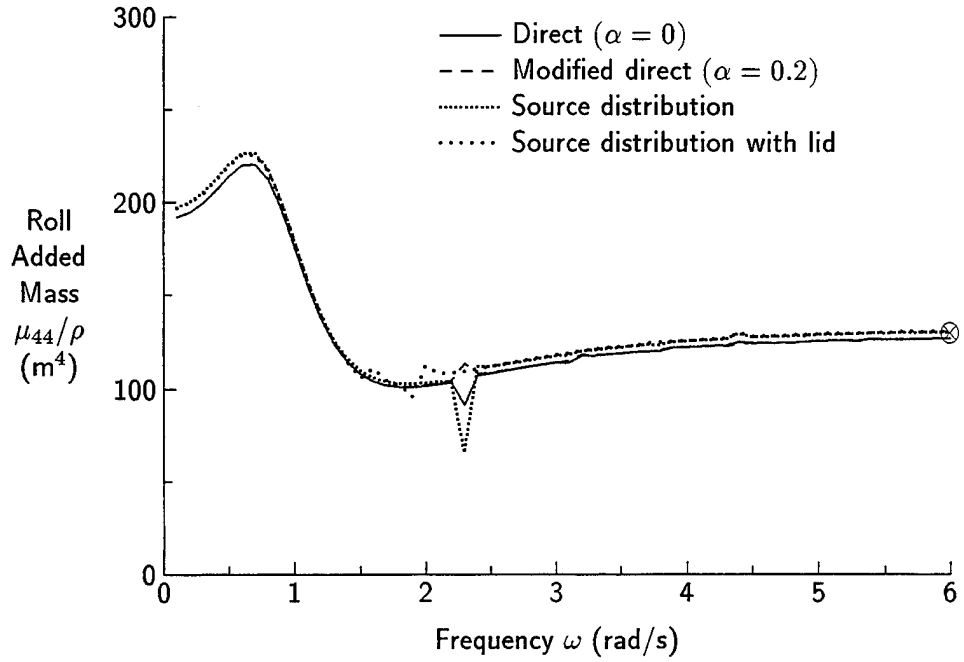

Figure 26: Roll Added Mass for Midship Section

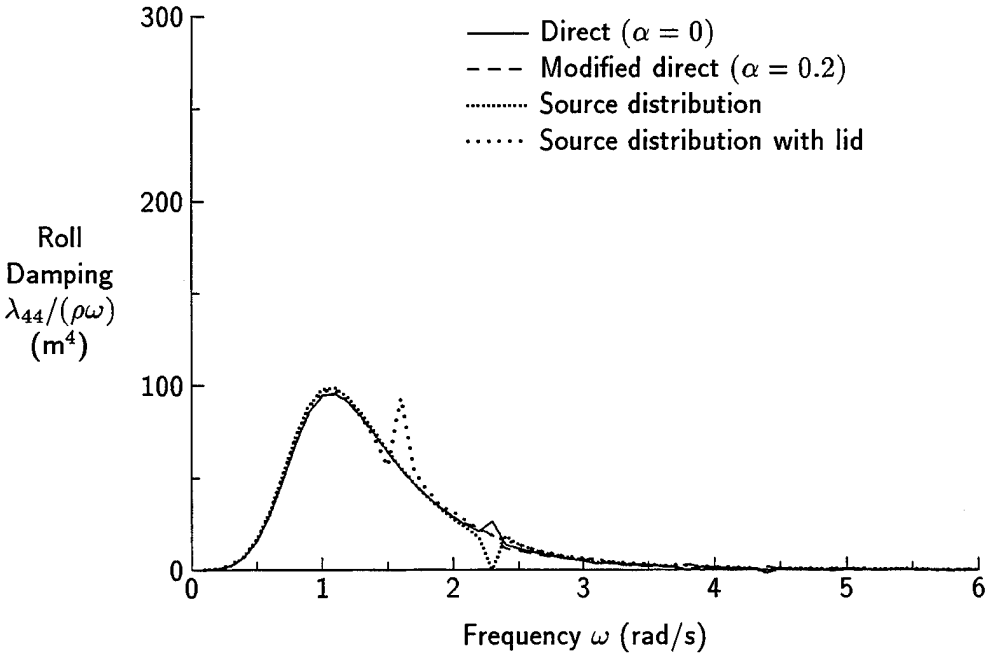

Figure 27: Roll Damping for Midship Section

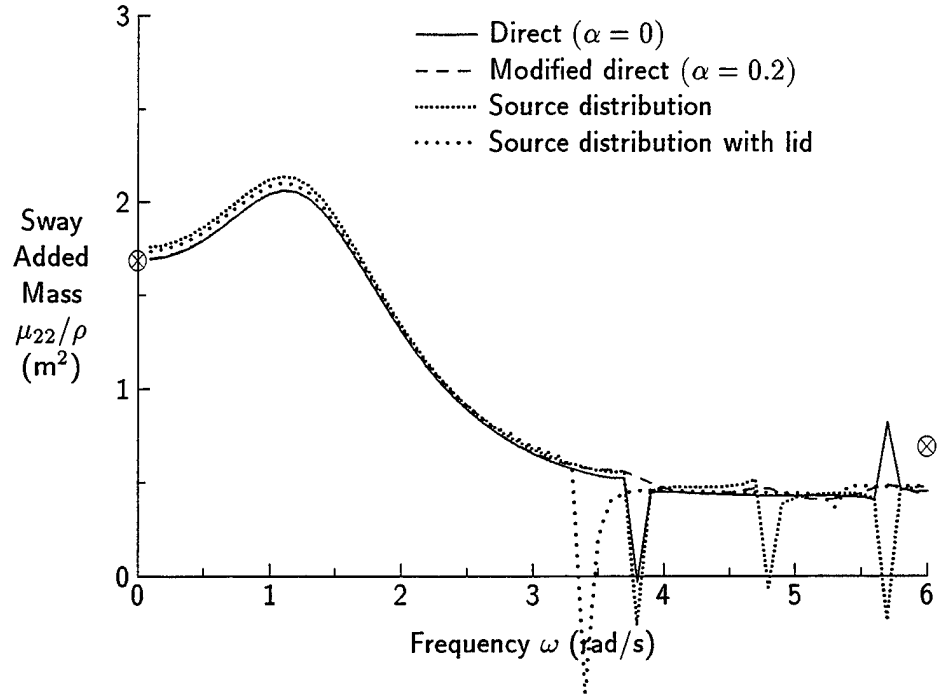

Figure 28: Sway Added Mass for Transom Section

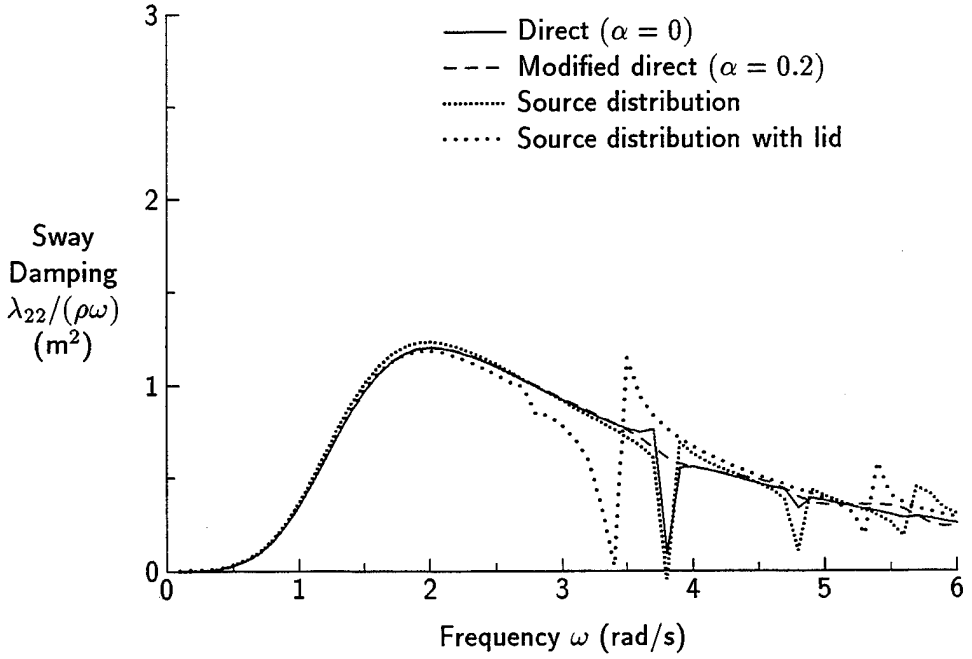

Figure 29: Sway Damping for Transom Section

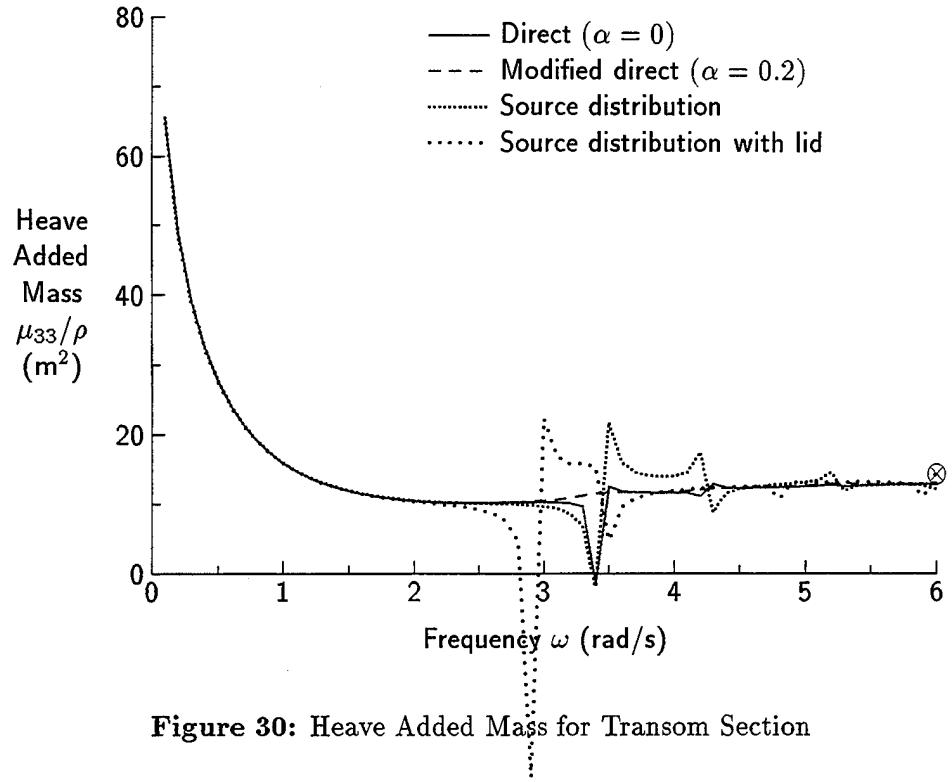

Figure 30: Heave Added Mass for Transom Section

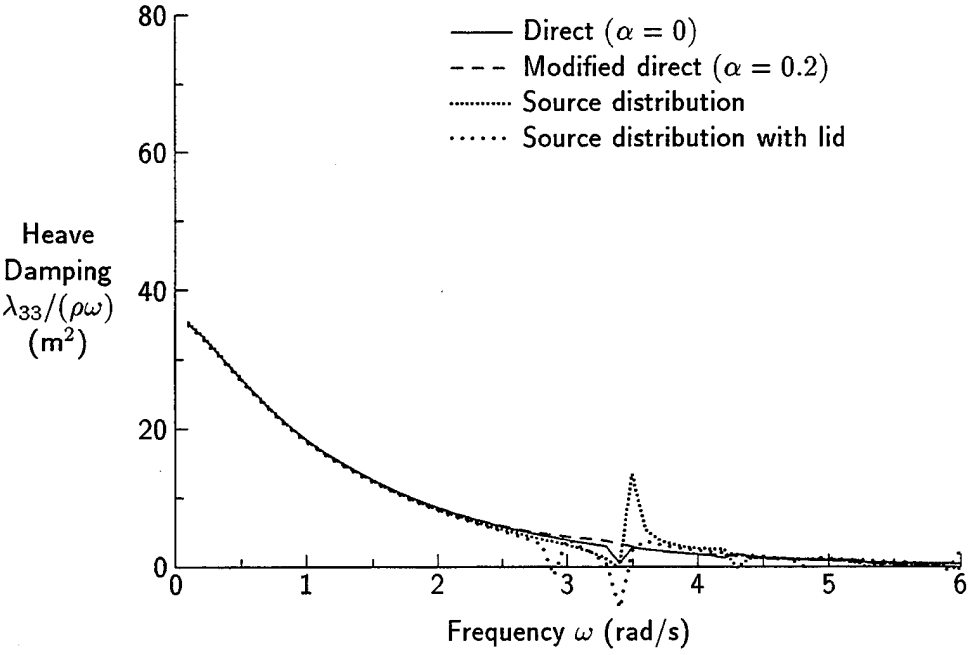

Figure 31: Heave Damping for Transom Section

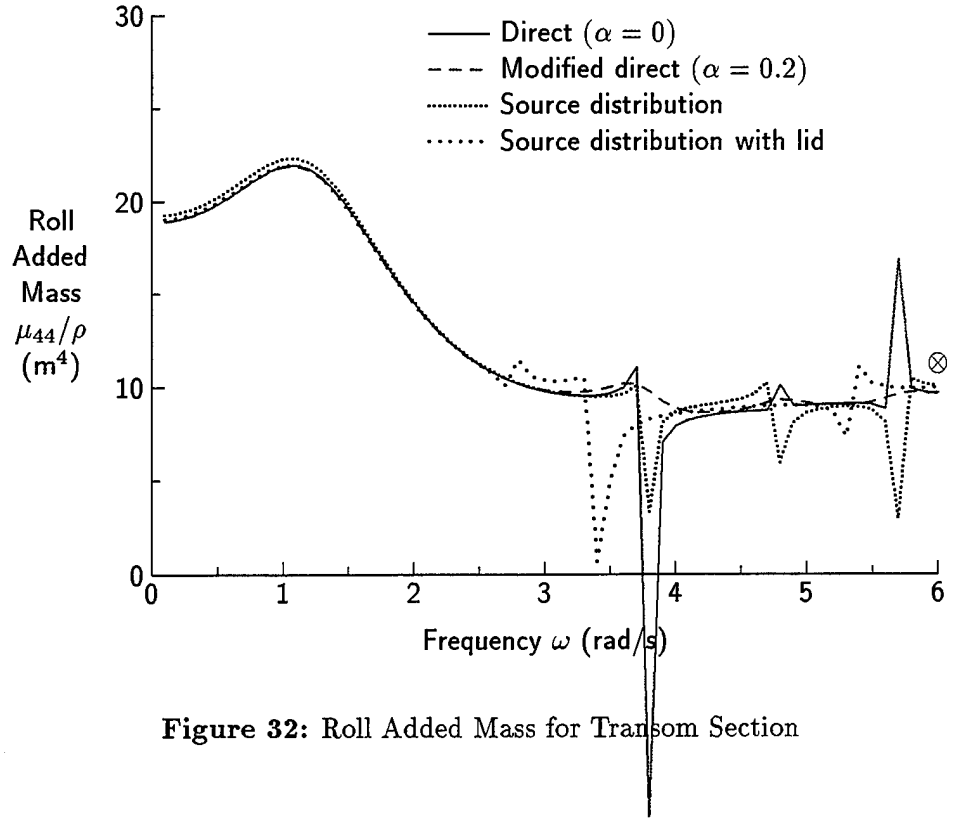

Figure 32: Roll Added Mass for Transom Section

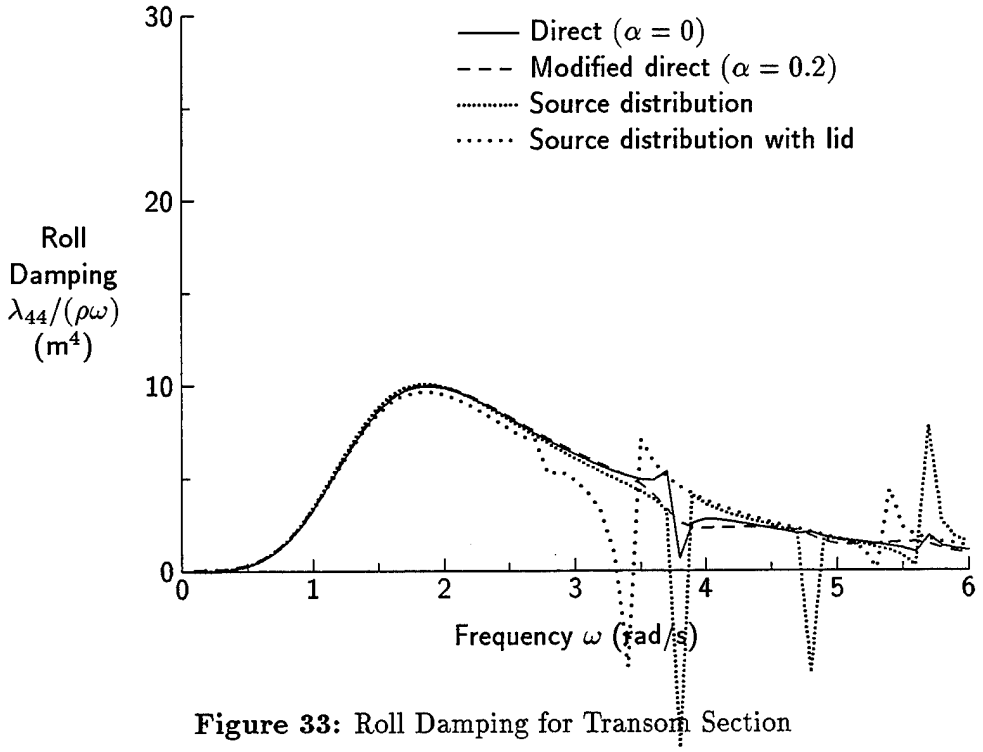

Figure 33: Roll Damping for Transom Section

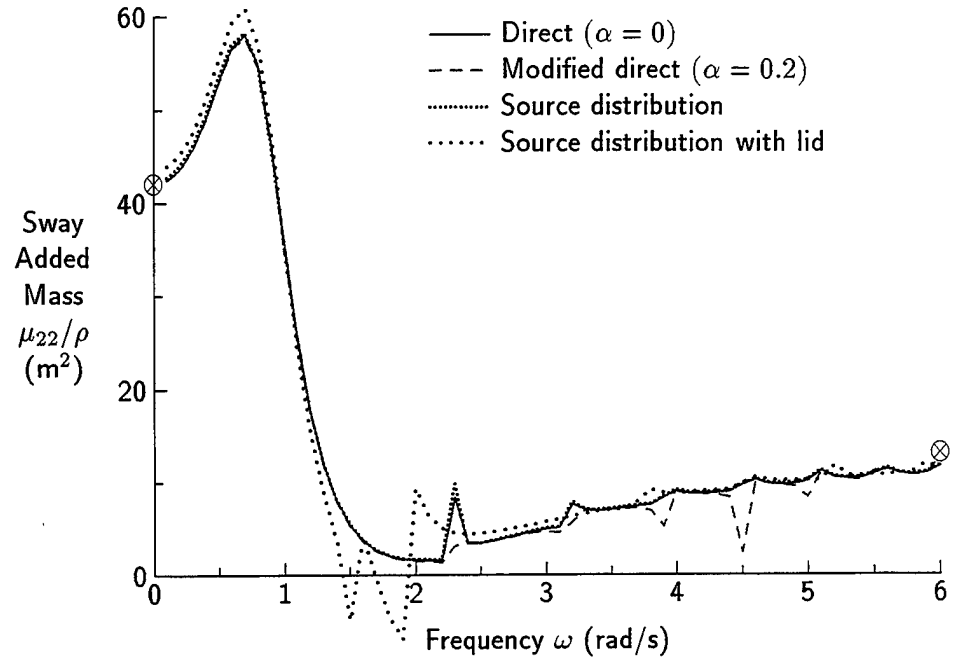

Figure 34: Sway Added Mass for Barge Section

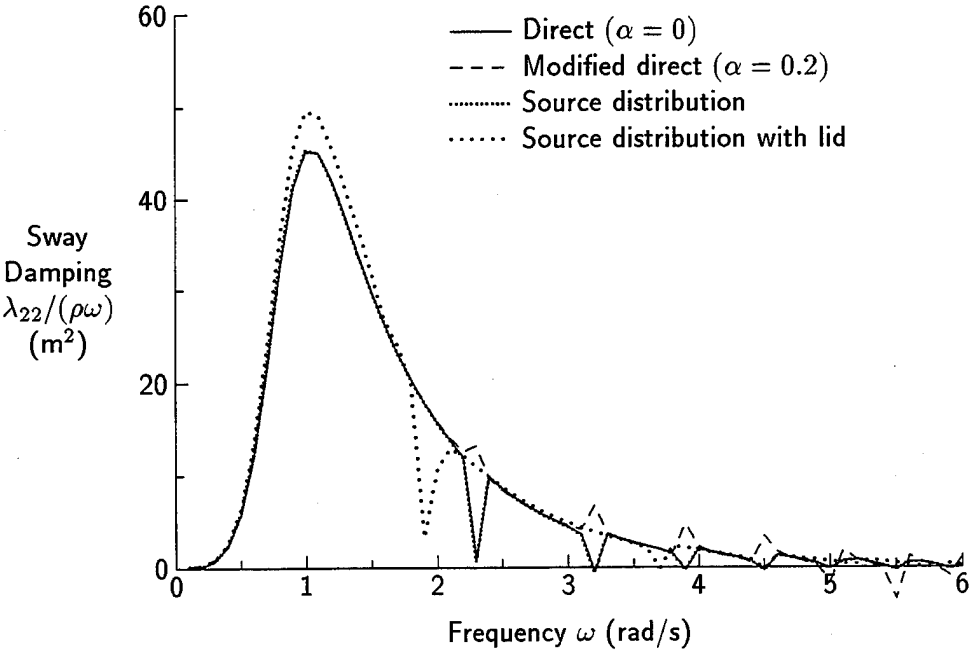

Figure 35: Sway Damping for Barge Section

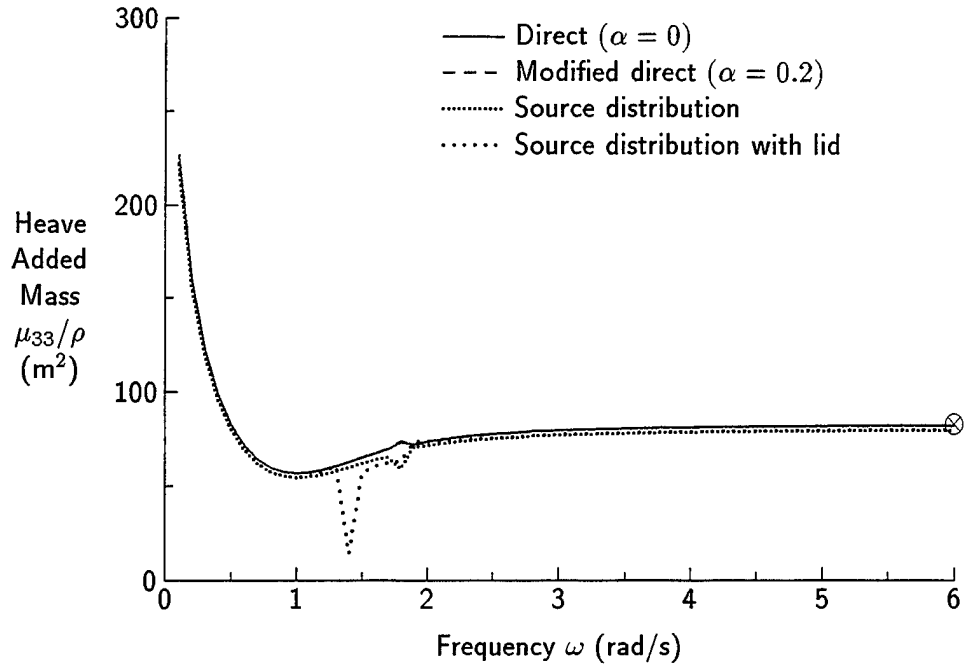

Figure 36: Heave Added Mass for Barge Section

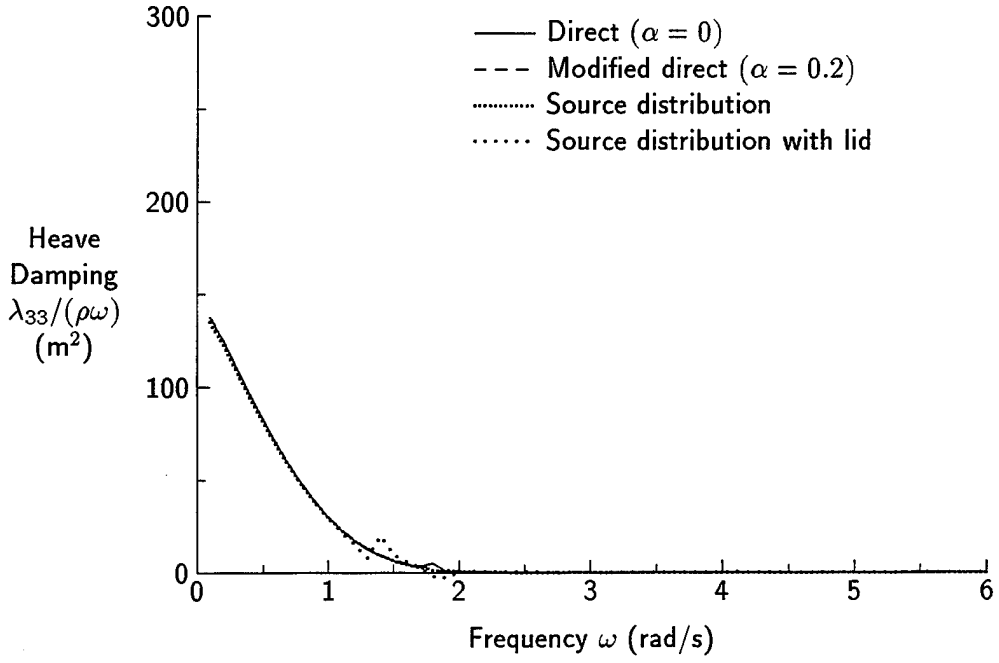

Figure 37: Heave Damping for Barge Section

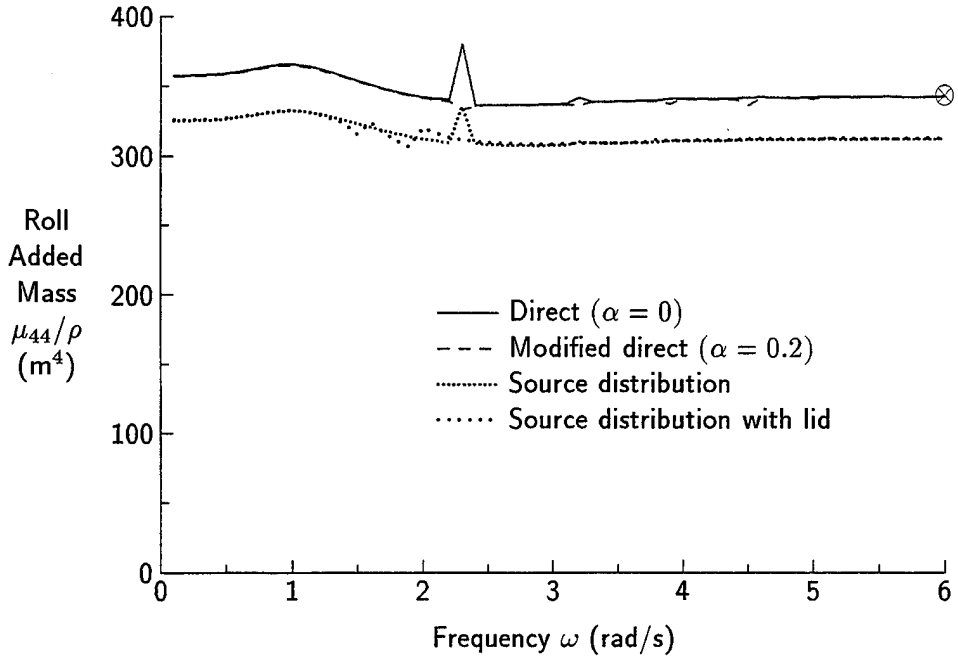

Figure 38: Roll Added Mass for Barge Section

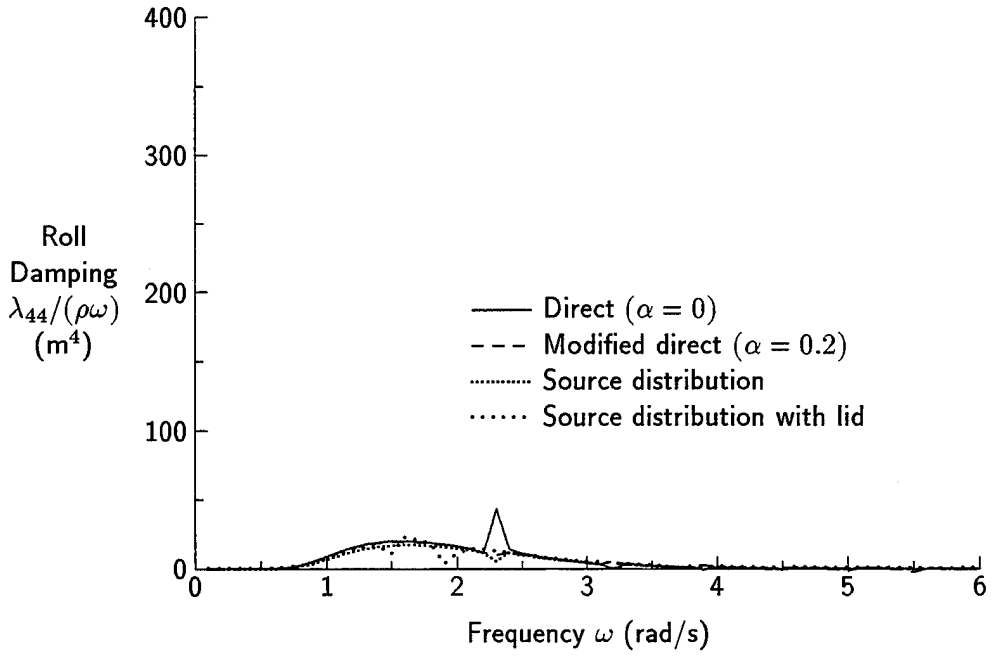

Figure 39: Roll Damping for Barge Section

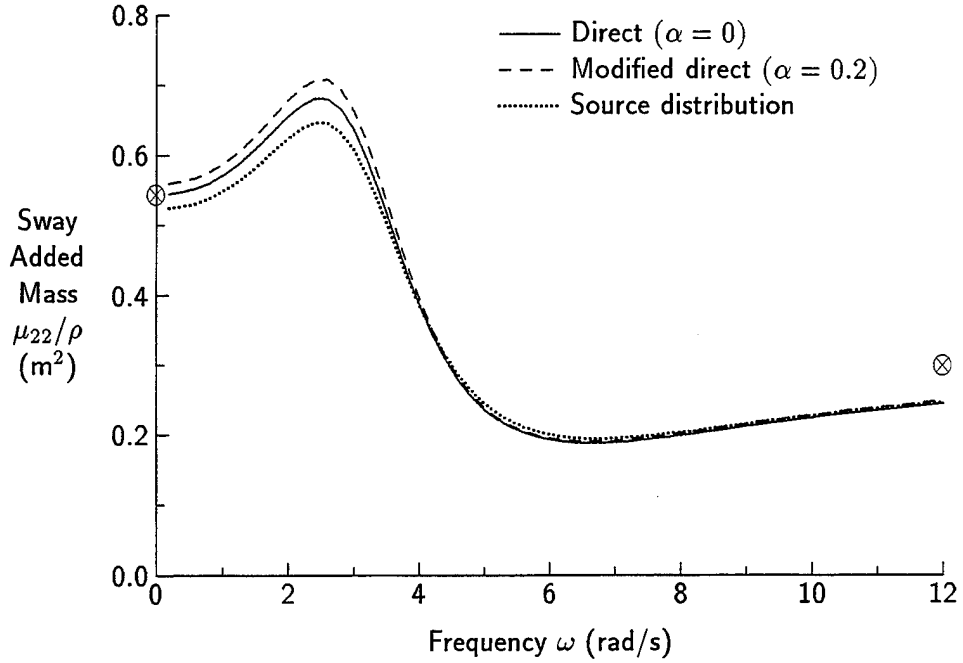

Figure 40: Sway Added Mass for Submarine Sail Section

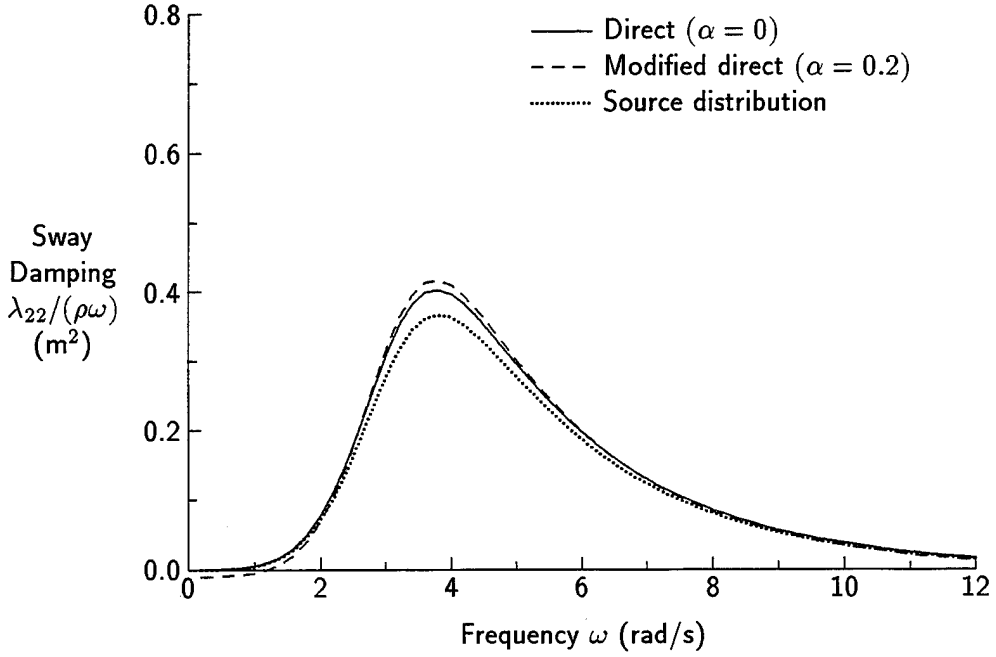

Figure 41: Sway Damping for Submarine Sail Section

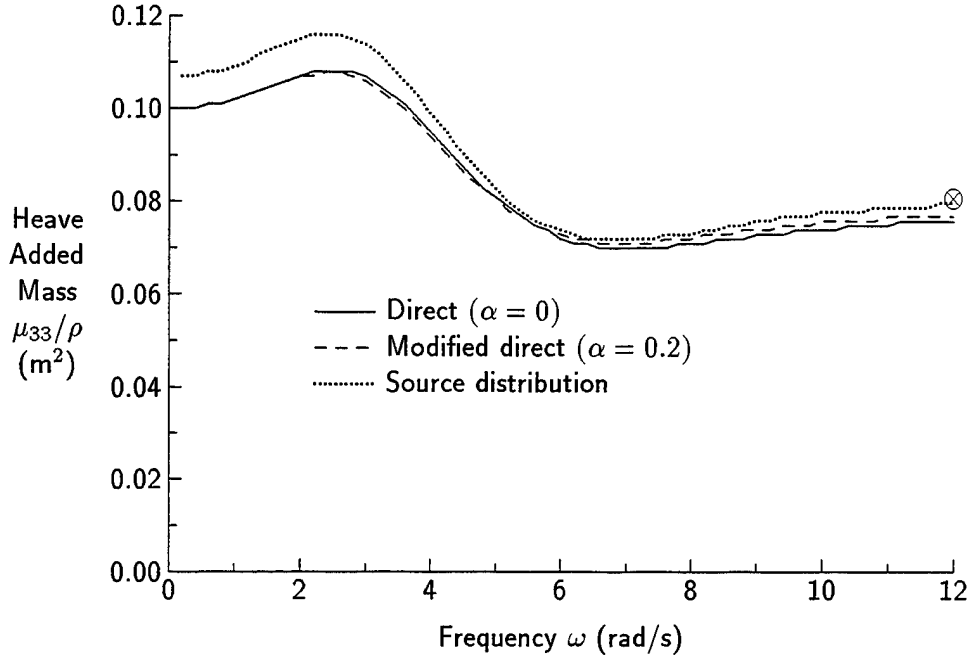

Figure 42: Heave Added Mass for Submarine Sail Section

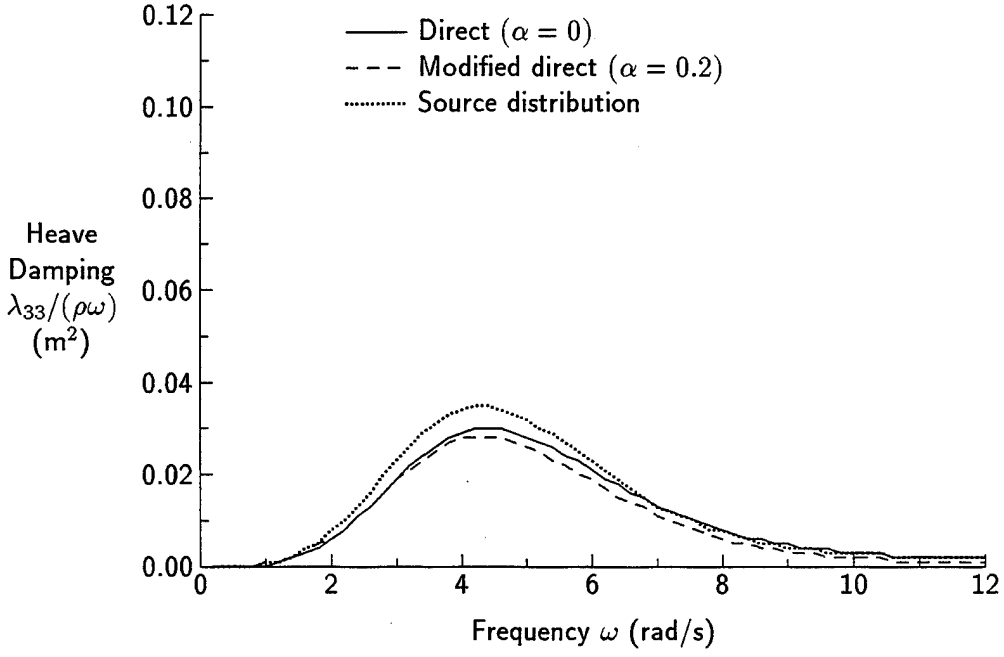

Figure 43: Heave Damping for Submarine Sail Section

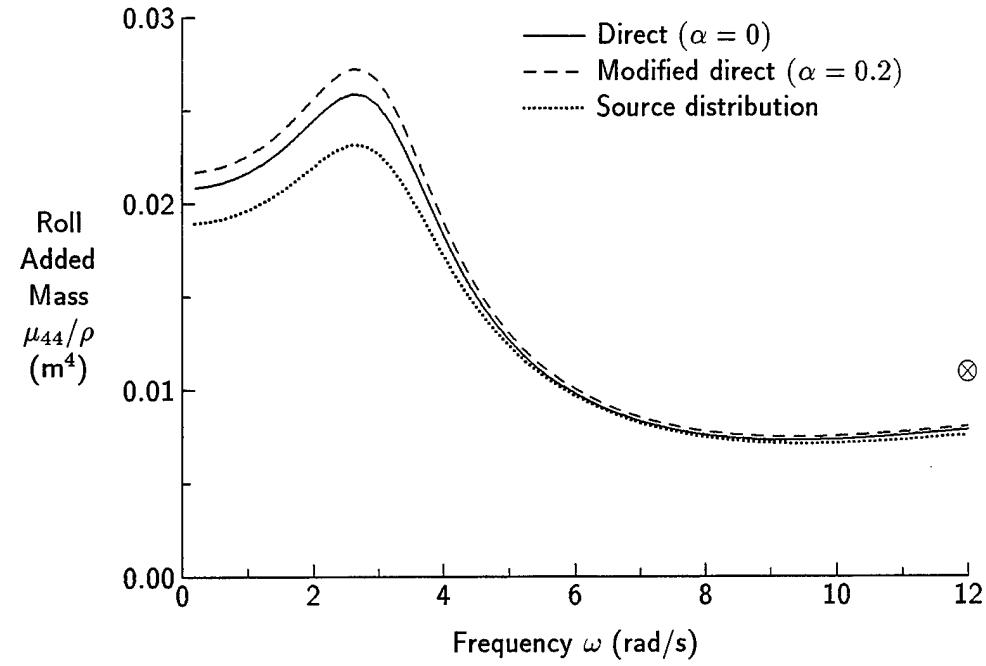

Figure 44: Roll Added Mass for Submarine Sail Section

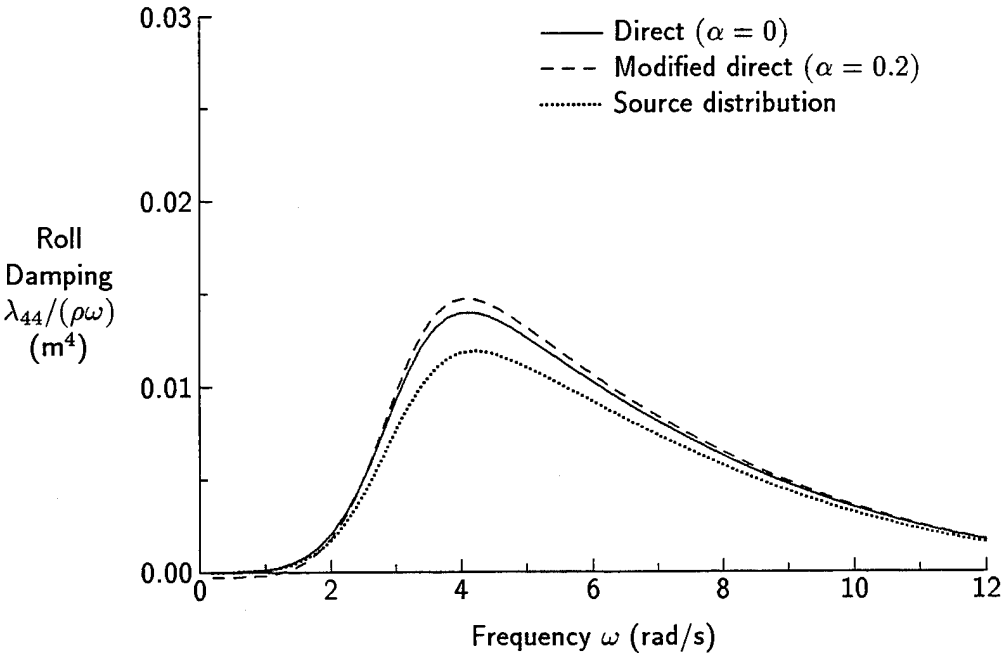

Figure 45: Roll Damping for Submarine Sail Section

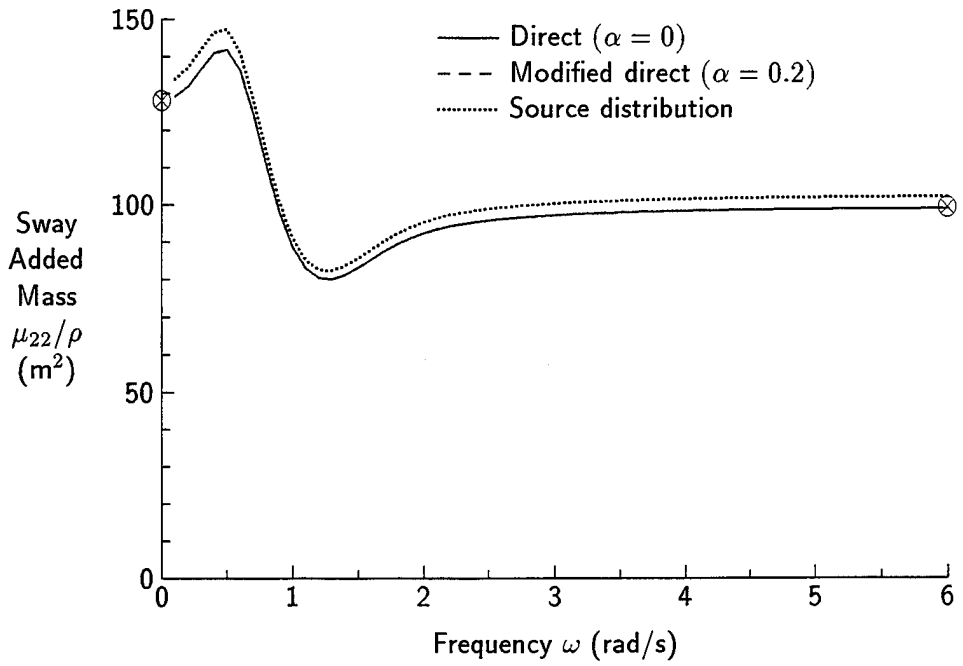

Figure 46: Sway Added Mass for Deep Circle Section

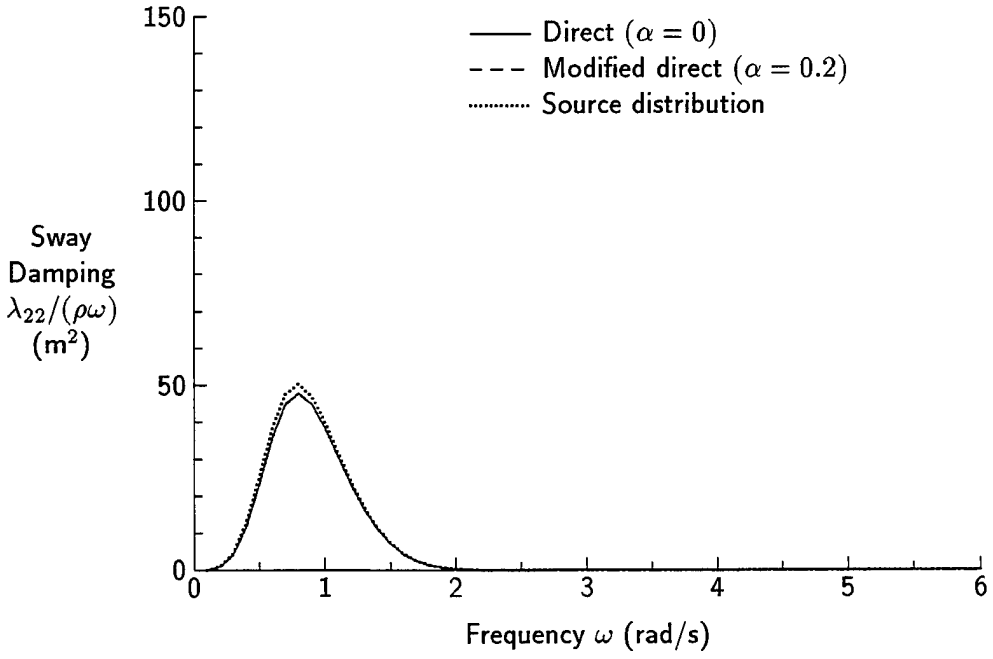

Figure 47: Sway Damping for Deep Circle Section

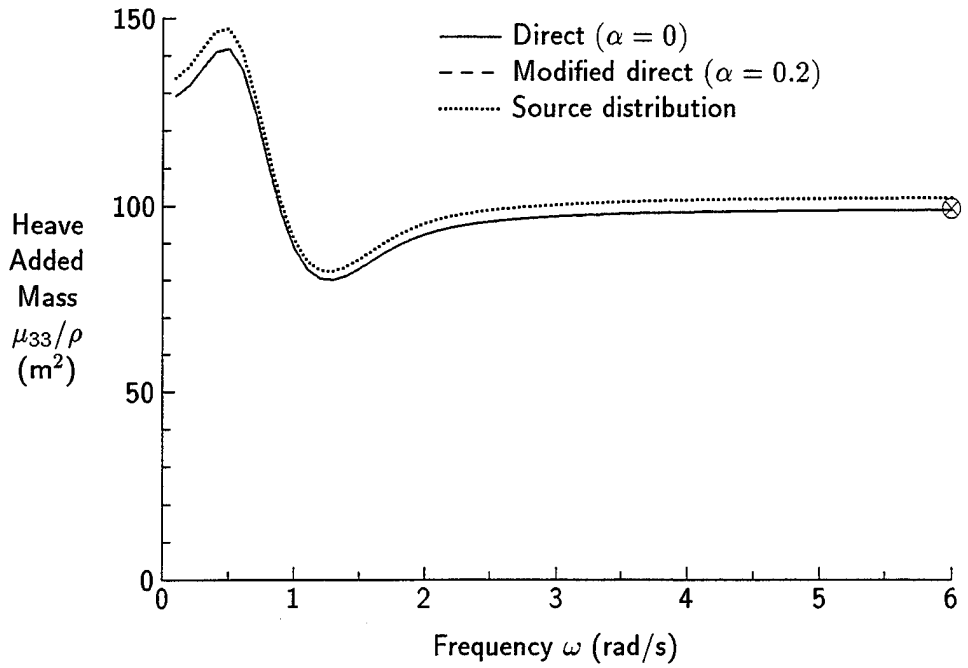

Figure 48: Heave Added Mass for Deep Circle Section

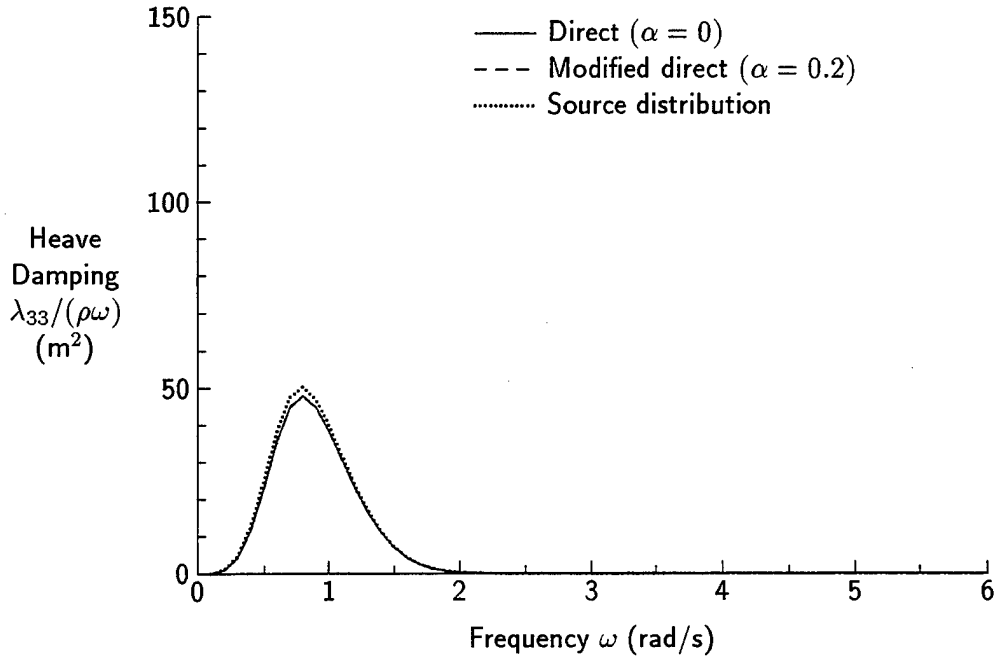

Figure 49: Heave Damping for Deep Circle Section

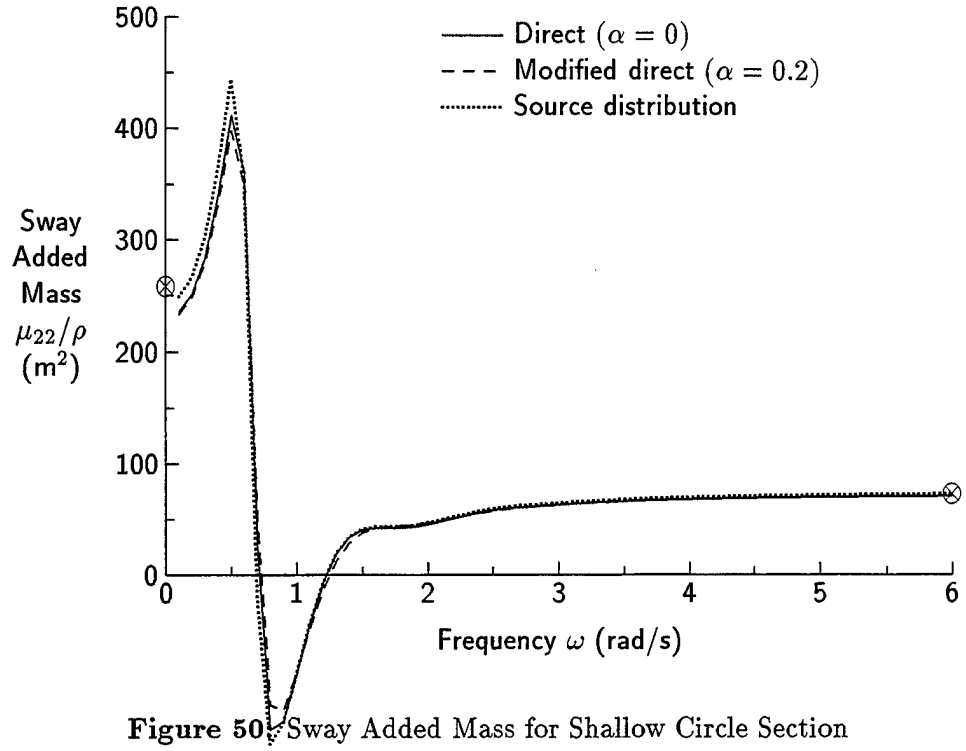

Figure 50: Sway Added Mass for Shallow Circle Section

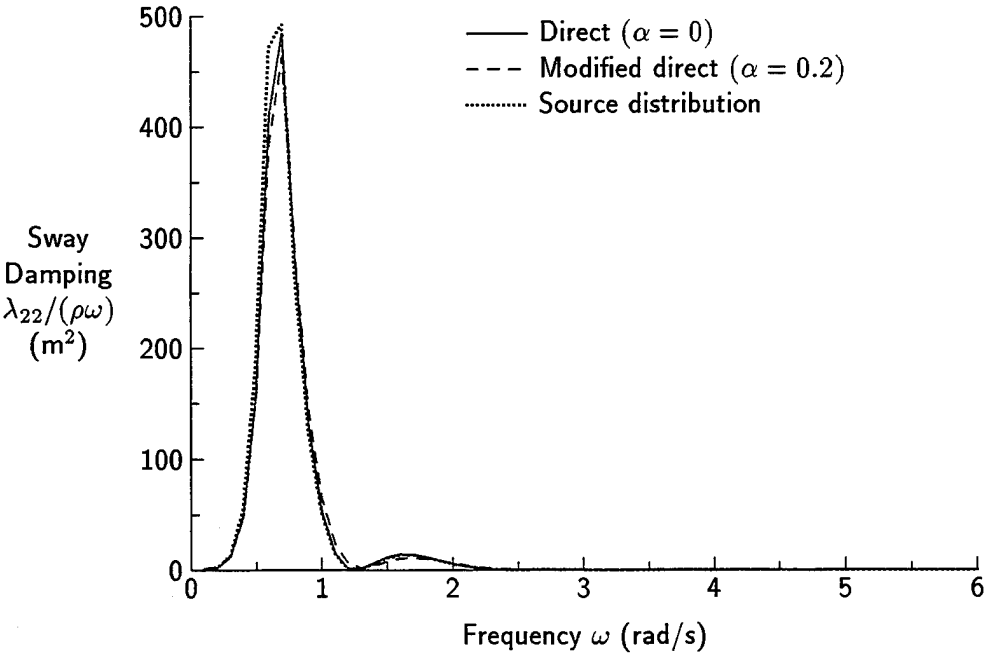

Figure 51: Sway Damping for Shallow Circle Section

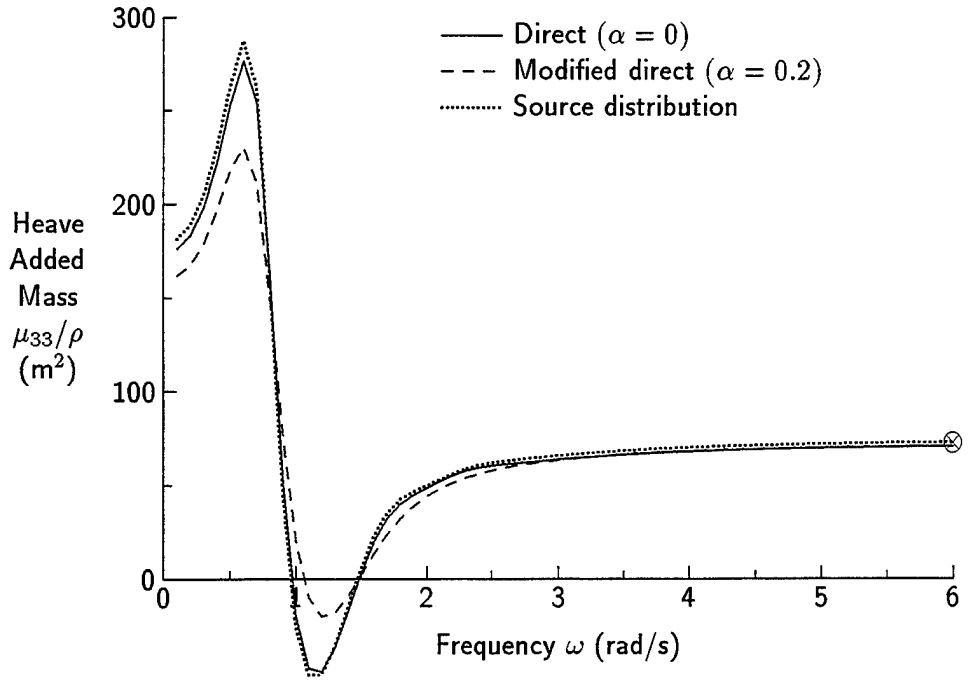

Figure 52: Heave Added Mass for Shallow Circle Section

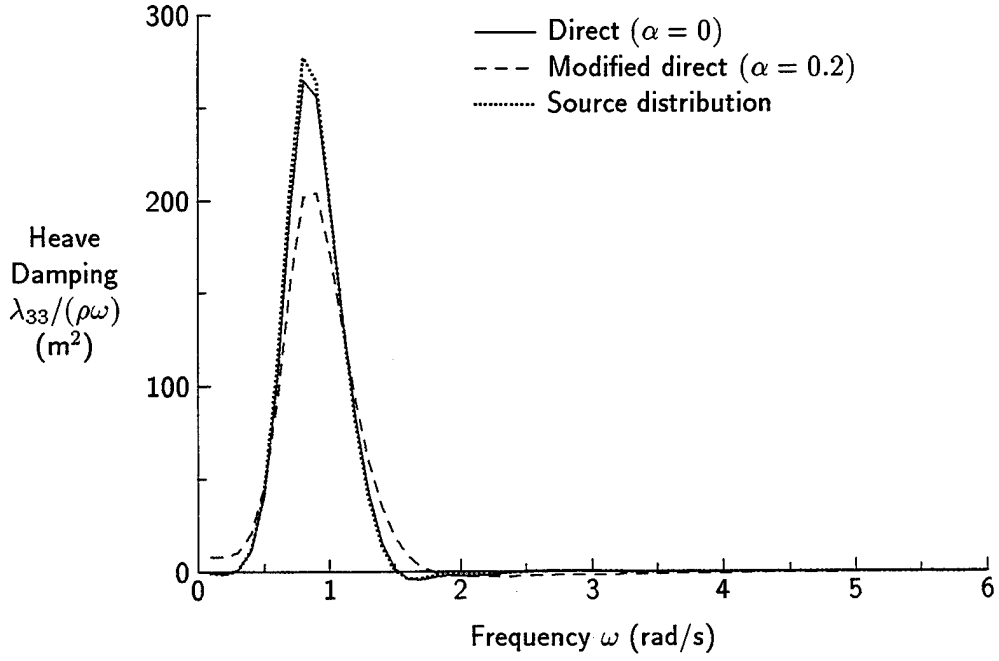

Figure 53: Heave Damping for Shallow Circle Section

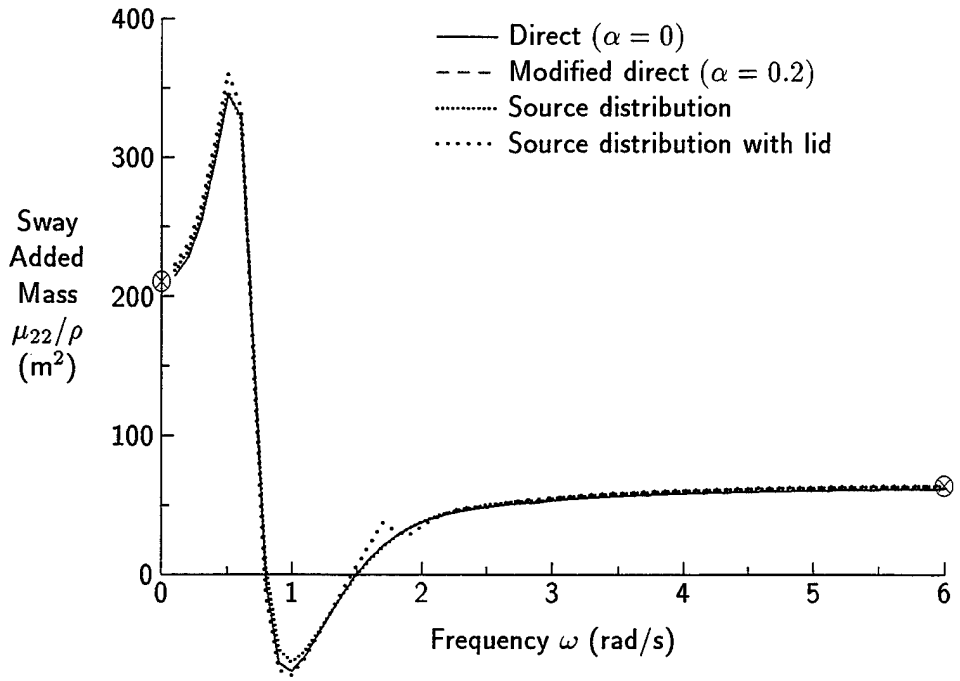

Figure 54: Sway Added Mass for Surface-Piercing Circle Section

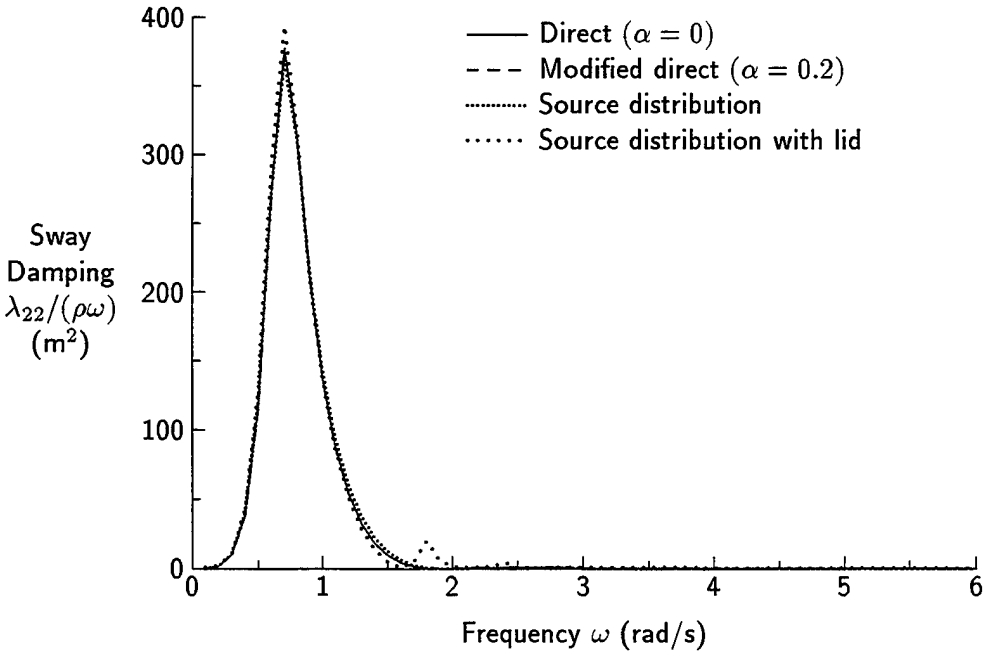

Figure 55: Sway Damping for Surface-Piercing Circle Section

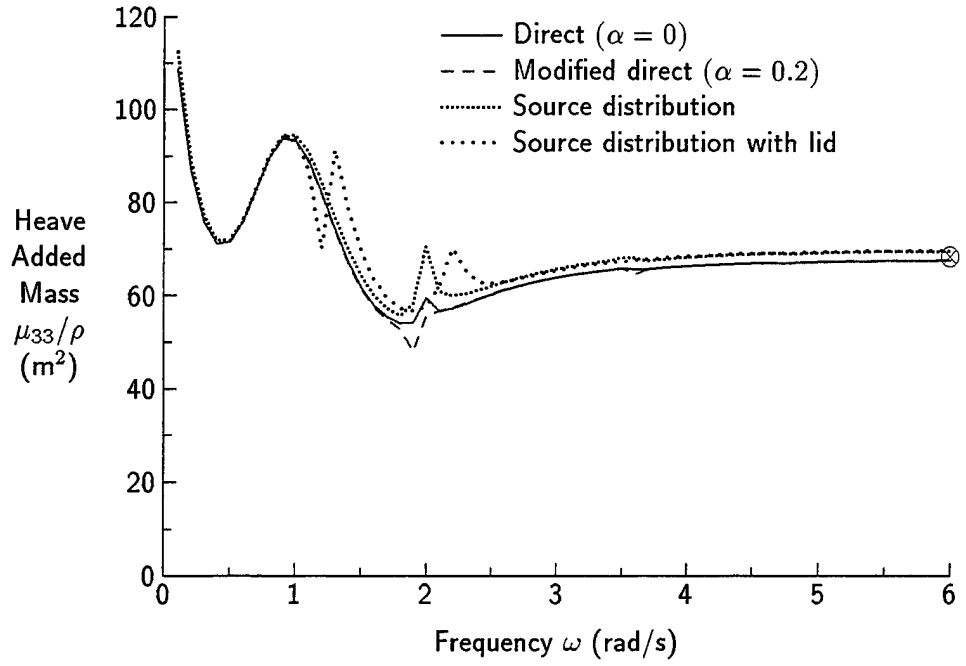

Figure 56: Heave Added Mass for Surface-Piercing Circle Section

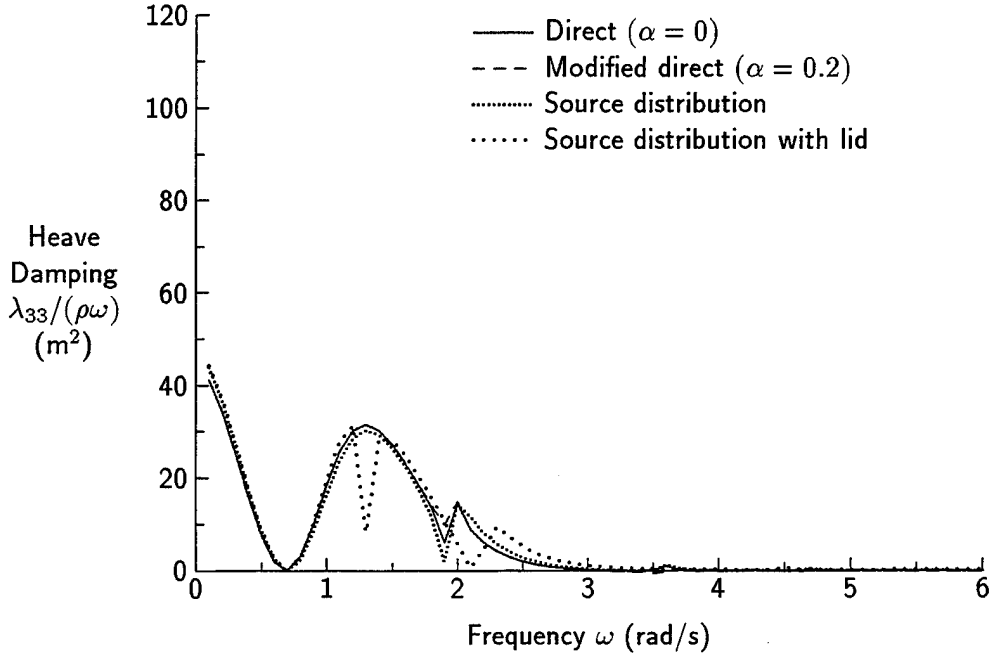

Figure 57: Heave Damping for Surface-Piercing Circle Section

8.3 Discussion of Computed Hydrodynamic Coefficients

In general, the computed hydrodynamic coefficients behave as expected, with good agreement between the direct and source distribution methods. The modified direct method clearly gives the most reliable results. The direct method ($\alpha = 0$) gives generally good results, but has some problems with irregular frequencies. The source distribution methods have problems regardless of whether a lid is used; the presence of a lid shifts the irregular frequencies. Irregular frequencies are particularly severe for the transom section, which has a high breadth to draft ratio.

The shallow and surface-piercing circle sections exhibit negative sway added mass. The consistency of the results suggests that these negative added masses could be a real physical phenomenon.

The zero and infinite frequency approximations for added mass show excellent agreement with the low and high frequency behaviour of the frequency dependent added masses. As oscillation frequency approaches zero, heave added mass of surface-piercing sections approaches infinity. In contrast, Kim [29] shows that heave added mass for semi-submerged ellipsoids approach finite limits as frequency approaches zero. The conclusion from this discrepancy is that two dimensional calculations greatly over-predict the heave added mass of a ship section at low frequency. The next section proposes a solution to this problem.

Unlike the close-fit method currently in SHIPMO, the new source distribution and direct methods are able to handle sections with horizontal and vertical segments, as demonstrated by the consistent results for the barge section.

9 Heave and Roll Coefficients at Low Encounter Frequency

As discussed earlier, a zero frequency Green function provides a suitable approximation for sway coefficients at low encounter frequencies. Unfortunately, this low frequency approximation is not valid for heave and roll.

Figures 20 to 45 indicate that roll added mass approaches a finite limit and roll damping approaches zero as oscillation frequency approaches zero. This consistent behaviour suggests that the following approximations can be used for predicting roll velocity potential and associated coefficients at low frequency:

$$\phi^{(4)}(\omega) = \frac{\omega}{\omega_o^{(4)}} \, i \, \text{Imag}\left\{\phi^{(4)}(\omega_o^{(4)})\right\} \tag{9.1}$$

$$\mu_{24}(\omega) = \mu_{24}(\omega_o^{(4)}) \tag{9.2}$$

$$\mu_{44}(\omega) = \mu_{44}(\omega_o^{(4)}) \tag{9.3}$$

$$\lambda_{24}(\omega) = 0 \tag{9.4}$$

$$\lambda_{44}(\omega) = 0 \tag{9.5}$$

where $\omega_o^{(4)}$ is the lowest frequency for which roll coefficients have been computed. From an analysis of the computed hydrodynamic coefficients in Figures 18 to 57, it is suggested that $\omega_o^{(4)}$

should be 0.2 $\sqrt{g/r_{max}}$ or lower, where r_{max} is the maximum distance from the roll origin to a sectional offset point.

In contrast to roll added mass and damping, heave added mass for surface-piercing two dimensional sections approaches infinity and damping approaches a finite value at low frequency, as illustrated in Figures 18 to 57. Heave added masses for semi-submerged ellipsoids presented by Kim [16] indicate that heave added mass approaches a finite zero frequency value and heave damping approaches zero at low frequency. Comparison of strip theory and three dimensional computations for semi-submerged ellipsoids in Figures 58 to 65 suggests that strip theory gives excessively high added mass and damping values for surface-piercing sections at low oscillation frequencies. The ellipsoids have draft equal to half the beam; thus, all sections are semi-circular. The ellipsoid with $L/B = 8$ can be considered a rough approximation of a frigate, while the ellipsoid $L/B = 4$ roughly approximates a coastal patrol vessel.

Strip theory should be able to provide reliable heave coefficient predictions for a slender ellipsoid (e.g. L/B = 8). Heave coefficient predictions for low L/B bodies, and pitch coefficient predictions for all bodies, are prone to errors caused by three dimensional effects. Examining the heave added mass and damping predictions in Figures 58 and 59 for the slender ellipsoid, it is proposed that sectional heave coefficients deteriorate when the oscillation frequency is below $\omega_o^{(3)} = 0.2\sqrt{g/y_{max}}$, where $\omega_o^{(3)}$ is the lowest frequency for reliable heave coefficients and y_{max} is maximum half-breadth of a given section. The cut-off frequency is referenced to y_{max} instead of y at the surface to account for sections which are narrow at the waterline but are significantly wider immediately below the surface.

Heave computations at $\omega_o^{(3)}$ can likely provide improved modelling of low frequency behaviour for an actual ship. The approximating equations are as follows:

$$\phi^{(3)}(\omega) = \frac{\omega}{\omega_o^{(3)}} \, i \, \text{Imag}\left\{\phi^{(3)}(\omega_o^{(3)})\right\} \tag{9.6}$$

$$\mu_{33}(\omega) = \mu_{33}(\omega_o^{(3)}) \tag{9.7}$$

$$\lambda_{33}(\omega) = 0 \tag{9.8}$$

Corrected strip theory coefficients in Figures 58 to 65 indicate that the low frequency heave correction leads to improved strip theory values.

10 Implementation of Improved Methods into Strip Theory Program SHIPMO

The modified direct method should replace the close-fit method presently used in SHIPMO in order to remove erratic results caused by irregular wave frequencies. It would also eliminate problems caused by vertical and horizontal section segments.

Appendix A gives documentation for the subroutine BOUND2D, which is the Fortran implementation of the direct method. Subroutine BOUND2D and various supporting routines can replace subroutine CLOSEFIT in the SHIPMO code. Integration of BOUND2D within the code should be quite simple. Velocity potentials from BOUND2D are the complex conjugate of

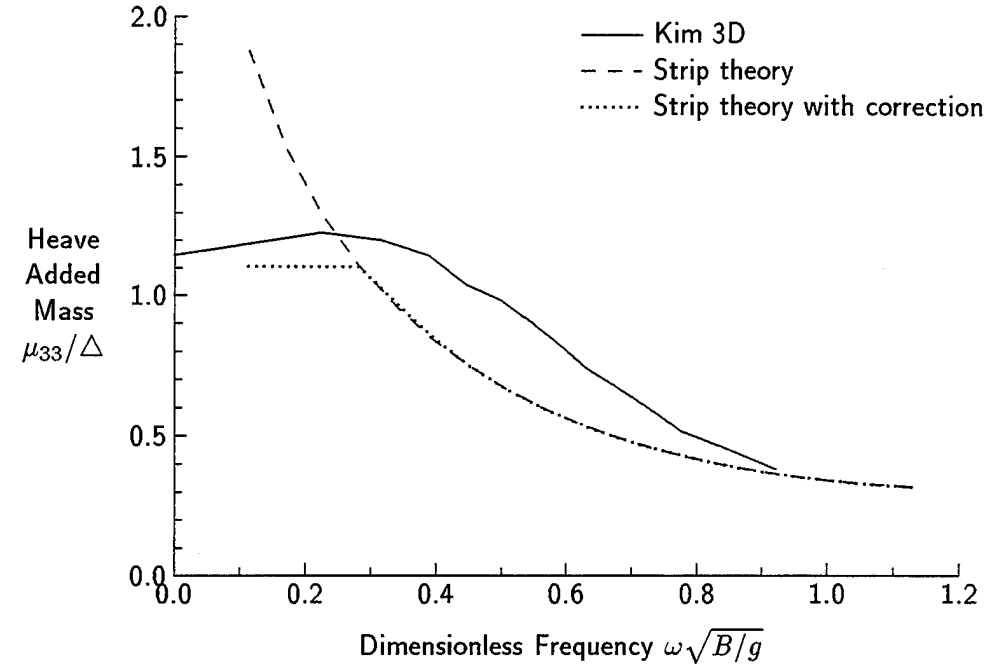

Figure 58: Heave Added Mass for Semi-Submerged Ellipsoid, $L/B = 8$

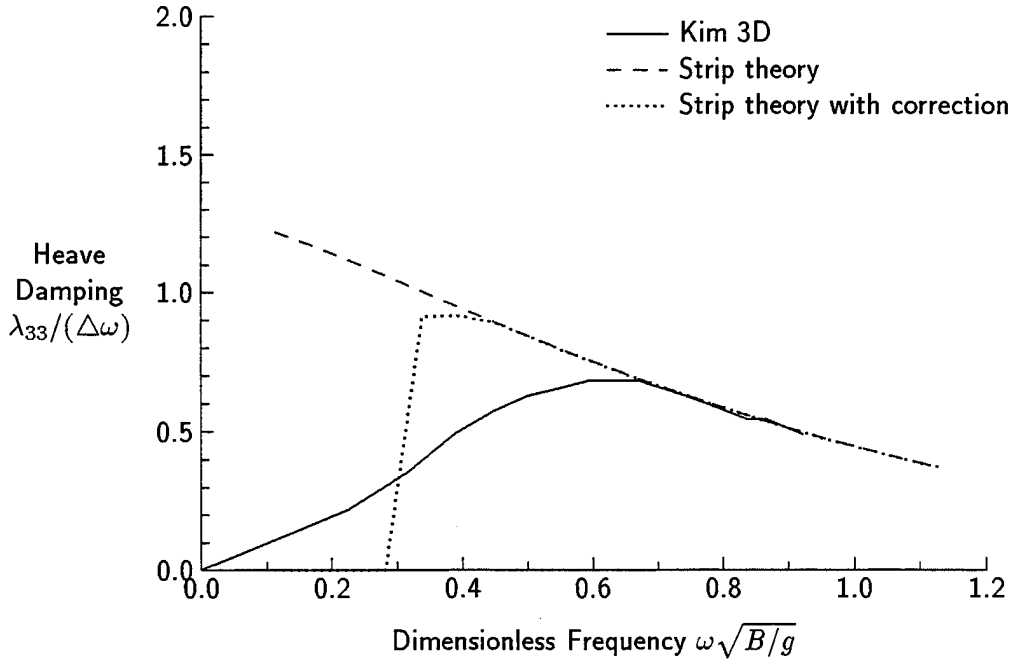

Figure 59: Heave Damping for Semi-Submerged Ellipsoid, $L/B = 8$

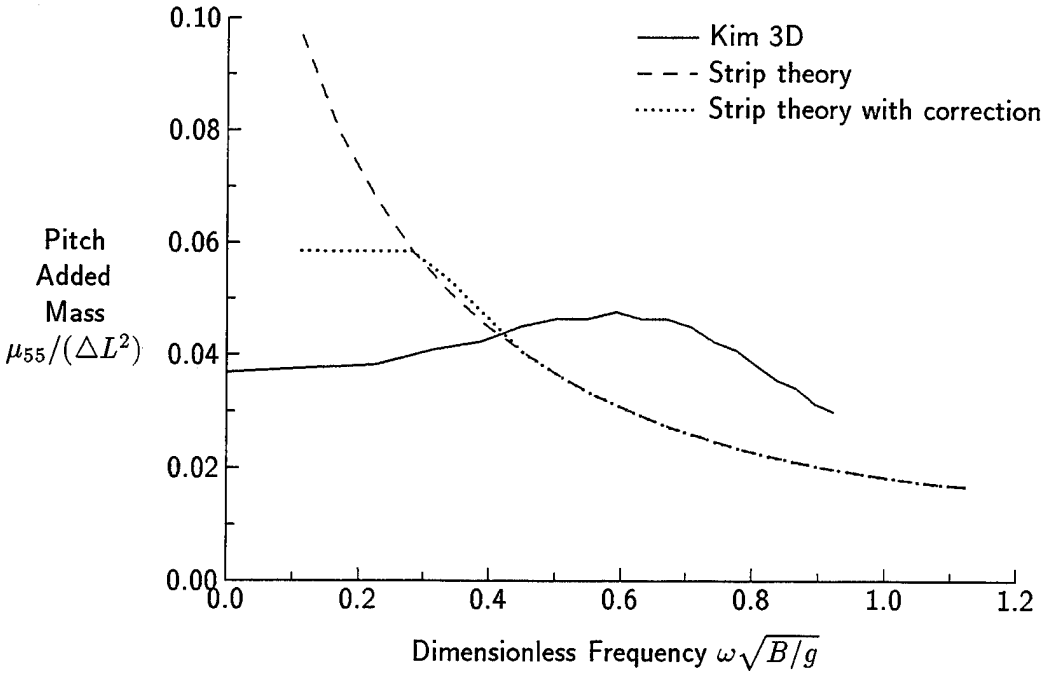

Figure 60: Pitch Added Mass for Semi-Submerged Ellipsoid, $L/B = 8$

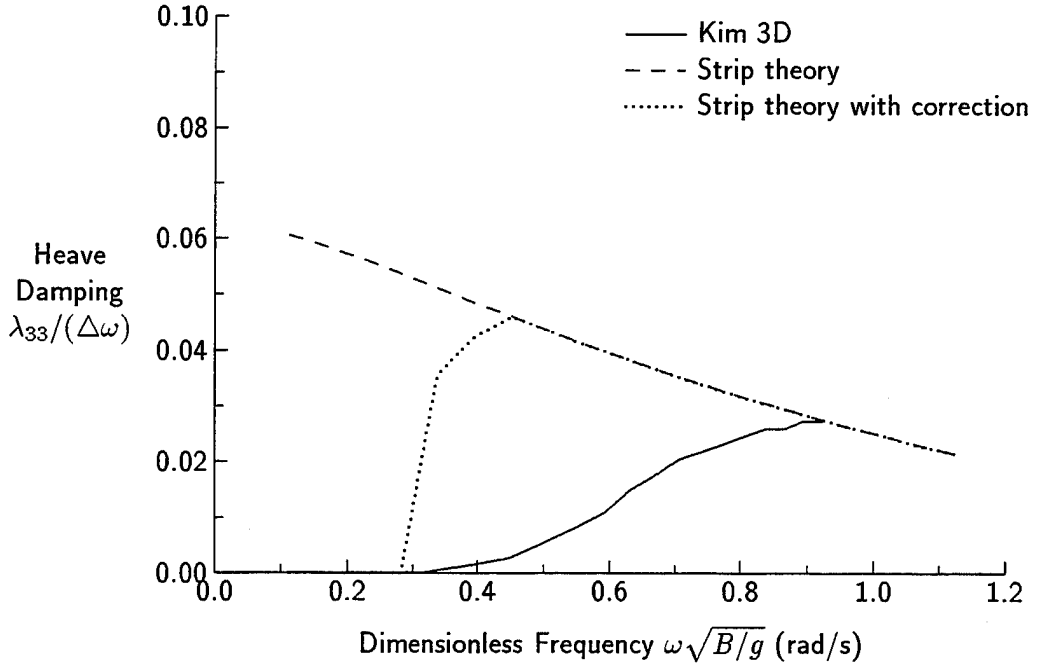

Figure 61: Pitch Damping for Semi-Submerged Ellipsoid, $L/B = 8$

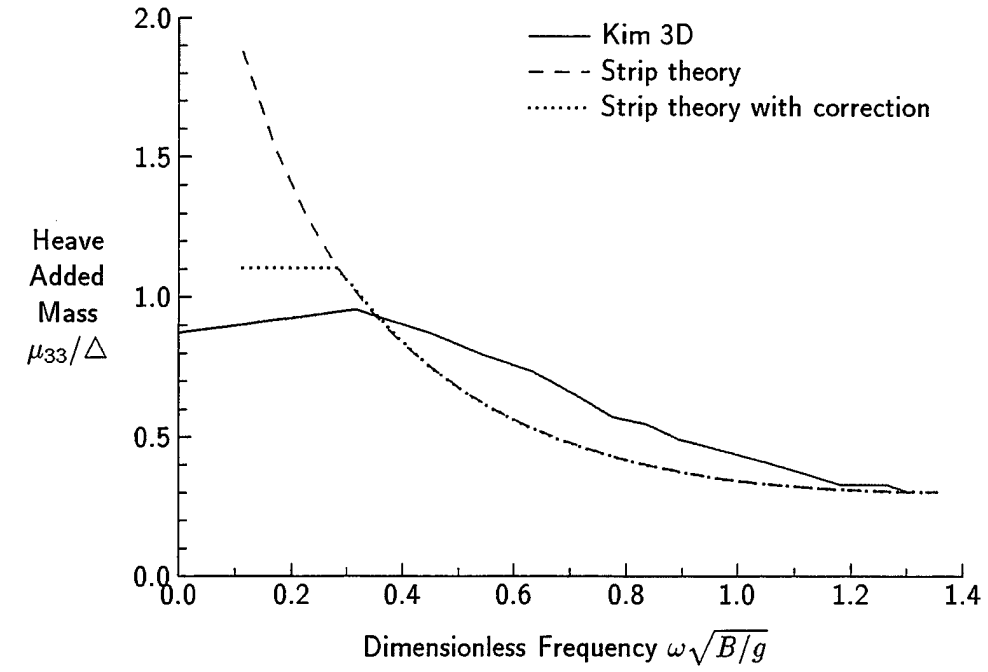

Figure 62: Heave Added Mass for Semi-Submerged Ellipsoid, $L/B = 4$

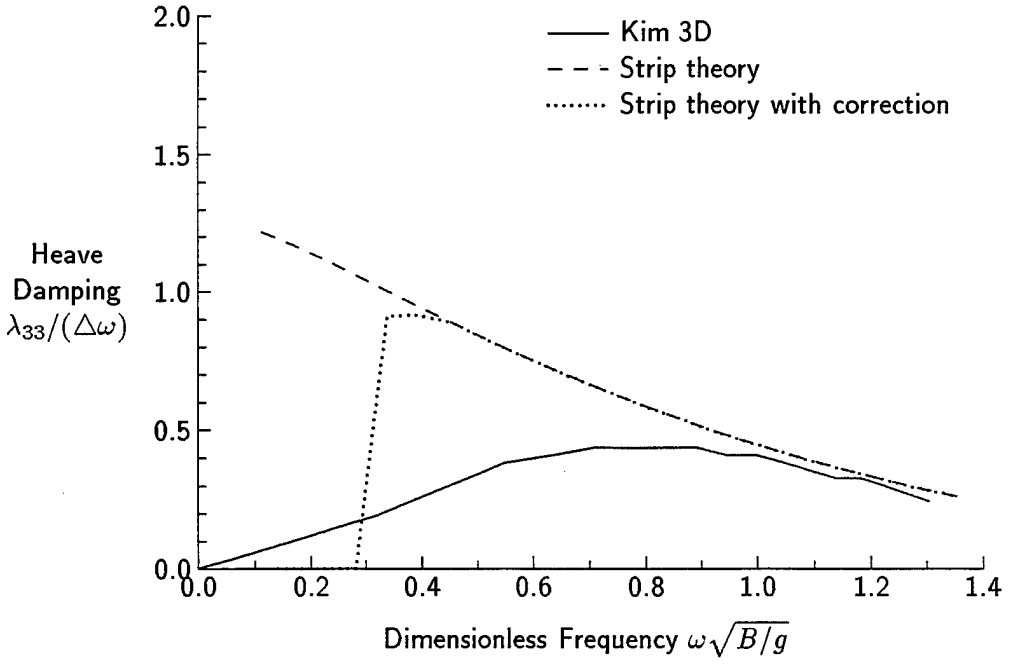

Figure 63: Heave Damping for Semi-Submerged Ellipsoid, $L/B = 4$

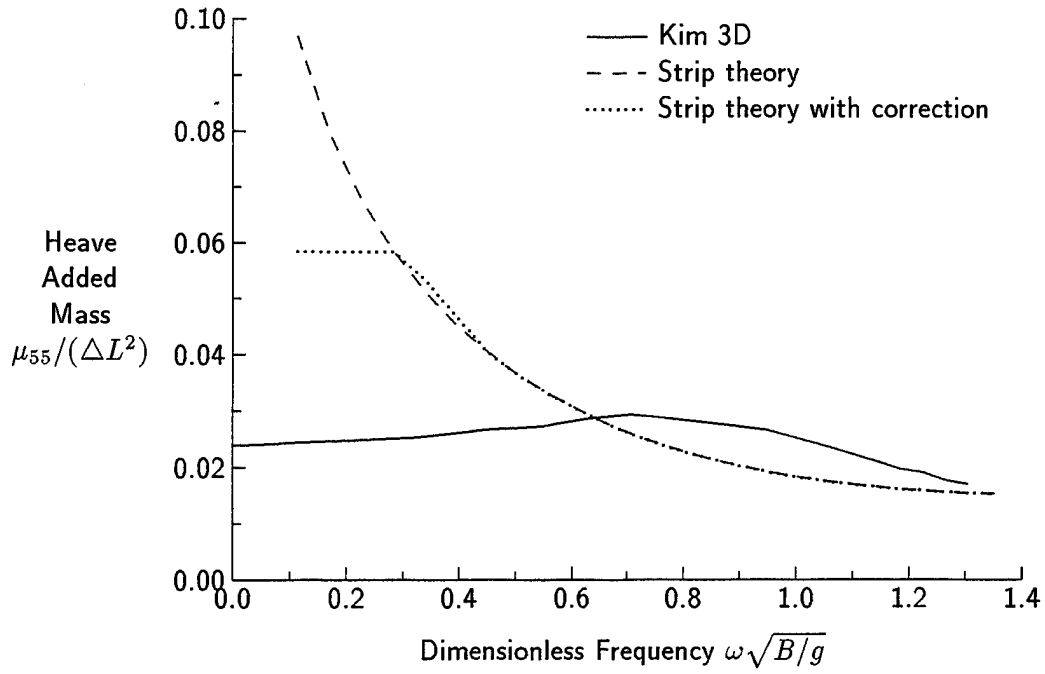

Figure 64: Pitch Added Mass for Semi-Submerged Ellipsoid, $L/B = 4$

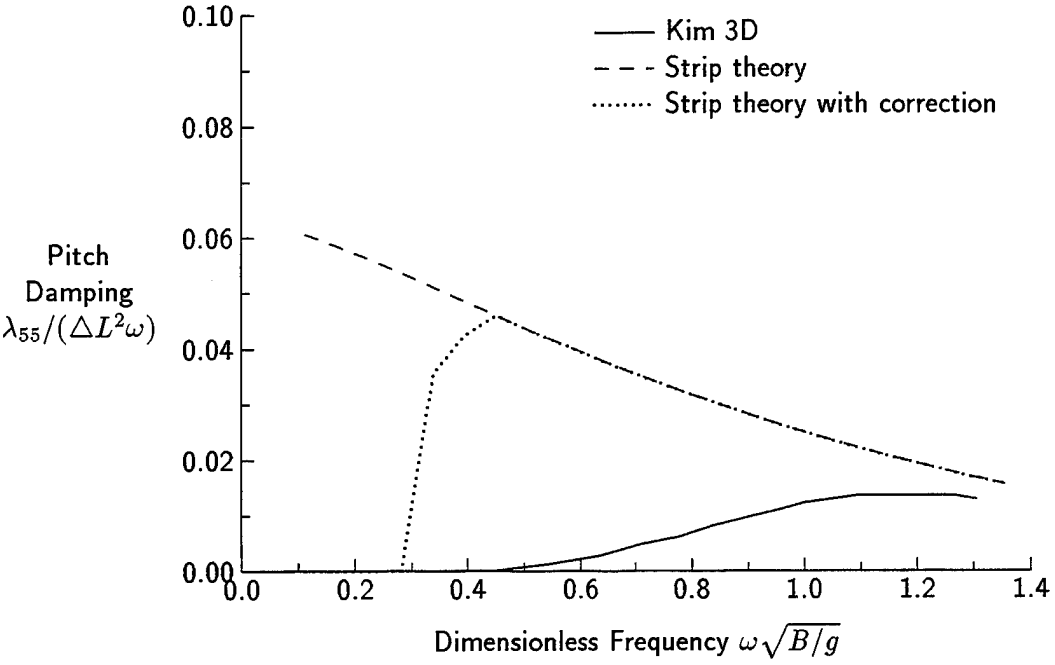

Figure 65: Pitch Damping for Semi-Submerged Ellipsoid, $L/B = 4$

values from CLOSEFIT. The present SHIPMO code calculates the complex conjugate of velocity potentials after calling CLOSEFIT; this step will not be necessary when BOUND2D replaces CLOSEFIT because the BOUND2D formulation is consistent with the rest of the SHIPMO code.

At high encounter frequencies, the approximation based on the infinite frequency Green function should be used to compute hydrodynamic coefficients for sway, heave, and roll. For sway at low encounter frequencies, SHIPMO can use an approximation based on the zero frequency Green function. For heave and roll at low encounter frequencies, SHIPMO can reasonably assume that velocity potential is proportional to frequency; however, the reference low frequency limit for heave must be carefully chosen. Furthermore, the influence of the heave low frequency approximation on excitation forces and ship motions should be examined before implementation into SHIPMO.

11 Conclusions

Two improved methods exist for predicting hydrodynamic coefficients of two dimensional sections. Of the two methods, the modified direct method gives more consistent results than the source distribution method. The modified direct method effectively eliminates problems caused by irregular frequencies.

Assymptotic solutions are available for sway, heave, and roll at high frequencies and for sway at low frequencies. Roll coefficients at low frequencies are well behaved. For low frequency heave of surface-piercing sections, two dimensional methods give unrealistically large values of added mass and damping for ship sections. A cut-off low frequency provides an improved estimate of added mass at low frequencies, and could possibly give improved motion predictions.

In the next revision of the SHIPMO strip theory code, the modified direct method should replace the existing close-fit method. This revision to SHIPMO will eliminate errors introduced by irregular frequencies. Low and high frequency approximations should also lead to improved SHIPMO predictions.

Appendix

A Subroutine BOUND2D for Computing Sectional Hydrodynamic Coefficients

Subroutine BOUND2D computes hydrodynamic coefficients for a two dimensional symmetrical ship section. The subroutine uses a modified direct method, which effectively eliminates problems caused by irregular frequencies for surface-piercing sections.

The Fortran declaration for the subroutine is:

```
 SUBROUTINE BOUND2D(IOLDGEOM, NP, YSECT, ZSECT, ZCG, GRAVITY, WE,
*              ALPHAB2D, AB2, AB24, AB3, AB4, PHI2, PHI3, PHI4)
 REAL YSECT(NP), ZSECT(NP)
 COMPLEX AB2, AB24, AB3, AB4, PHI2(NP-1), PHI3(NP-1), PHI4(NP-1)
```

The units of the input and output variables are determined by the value of GRAVITY (typically 9.806 m/s^2 or 32.174 ft/s^2). The input variables are:

IOLDGEOM	Set to 1 if same geometry as previous call to subroutine, 0 otherwise,
NP	Number of section offset points,
YSECT	Vector of NP lateral offsets (m or ft), beginning at keel (YSECT(I) $\geq$ 0),
ZSECT	Vector of NP vertical offsets (m or ft) relative to waterline, beginning at keel (ZSECT(I) $\leq$ 0),
ZCG	Height of reference point above waterline (m or ft),
GRAVITY	Gravitational acceleration (m/s^2 or ft/s^2). GRAVITY is typically 9.806 (metric) or 32.174 (British).
WE	Encounter frequency (rad/s).

The hydrodynamic coefficients must be multiplied by water density to get added mass and damping. The output variables are:

AB2	Real component is sway added mass (m^2 or ft^2) and imaginary component is sway damping (m^2/s or ft^2/s),
AB24	Real component is sway-roll added mass (m^3 or ft^3) and imaginary component is sway-roll damping (m^3/s or ft^3/s),
AB3	Real component is heave added mass (m^2 or ft^2) and imaginary component is heave damping (m^2/s or ft^2/s),
AB4	Real component is roll added mass (m^4 or ft^4) and imaginary component is roll damping (m^4/s or ft^4/s),

PHI2	Vector of sway velocity potentials on segments (m/s or ft/s),
PHI3	Vector of heave velocity potentials on segments (m/s or ft/s),
PHI4	Vector of roll velocity potentials on segments (m^2/s or ft^2/s).

References

1. R.T. Schmitke and B.W. Whitten, "SHIPMO - A FORTRAN Program to Predict Ship Motions in Waves," DREA Technical Memorandum 81/C, October 1981.

2. R. Graham and G. Miller, "SHIPMO2 - An Updated User's Manual for the SHIPMO Computer Program Incorporating Measured Sea Spectra and Wave Loads," DREA Technical Memorandum 84/G, May 1984.

3. R. Graham, "SHIPMO3: Improved Viscous Roll Damping Predictions for the SHIPMO Computer Program," DREA Technical Memorandum 86/212, May 1986.

4. R. Graham and C. Trudelle, "SHIPMO4 - An Updated User's Manual for the SHIPMO Computer Program Incorporating an Extended Hydrostatics Capability and an Improved Viscous Roll Damping Model," DREA Technical Communication 87/304, March 1987.

5. K.A. McTaggart and R. Graham, "SHIPMO5: An Updated User's Manual Incorporating New Wave Spectra and Ship-Referenced Forces," DREA Technical Memorandum 92/212, April 1992.

6. K.A. McTaggart, "SHIPMO6: An Updated Strip Theory Ship Motion Program," DREA Technical Memorandum 93/213, October 1993.

7. W. Frank, "Oscillation of Cylinders on or Below the Free Surface of Deep Fluids," Report 2305, Naval Ship Research and Development Center, October 1967.

8. W. Frank and N. Salvesen, "The Frank Close-Fit Ship-Motion Computer Program," Report 3289, Naval Ship Research and Development Center, June 1970.

9. O.M. Faltinsen, "A Study of the Two-dimensional Added-mass and Damping Coefficients by the Frank Close-fit Method," Report 69-10-S, Det Norske Veritas Research Department, 1969.

10. J.W. Bedel, "Improved Method for the Calculation of the Added Mass and Damping Coefficients of Oscillating Cylinders," Technical Note 216, Naval Ship Research and Development Center, November 1971.

11. S. Ohmatsu, "On the Irregular Frequencies in the Theory of Oscillating Bodies," *Papers of Ship Research Institute* (48) (1975).

12. S. Ando, "AMADIFF - A FORTRAN Routine for Irregular-Frequency-Free Calculation of Added Mass and Damping of Two-Dimensional Floating Bodies by the Extended Boundary Element Method," DREA Technical Memorandum 95/213, May 1995.

13. P.D. Sclavounos and C. Lee, "Topics on Boundary Element Solutions of Wave Radiation-Diffraction Problems," in *Fourth International Conference on Numerical Ship Hydrodynamics* (Washington, 1985).

14. G.W. Johnston and S.P. Foster, "Frequency Domain Prediction of Submarine Motion in Waves (SUBMO) – Volume 1," DREA Contractor Report CR/91/435, July 1991.

15. G.W. Johnston and A. Skarsgard, "Frequency Domain Prediction of Submarine Motion in Waves – SUBMO2 Final Report," DREA Contractor Report CR/93/438, July 1992. Limited Distribution.

16. W.D. Kim, "On the Harmonic Oscillations of a Rigid Body on a Free Surface," *Journal of Fluid Mechanics* **21** (1965).

17. T. Sarpkaya and M. Isaacson, *Mechanics of Wave Forces on Offshore Structures*, Van Nostrand Reinhold, 1981.

18. C.C. Mei, *The Applied Dynamics of Ocean Surface Waves*, John Wiley & Sons, New York, 1983.

19. J.N. Newman, "The Evaluation of Free-Surface Green Functions," in *Fourth International Conference on Numerical Ship Hydrodynamics* (Washington, 1985).

20. N. Salvesen, E.O. Tuck, and O. Faltinsen, "Ship Motions and Sea Loads," *Transactions, Society of Naval Architects and Marine Engineers* **78**, 250–287 (1970).

21. R.A. Comeau and S. Ando, "AMAD - A FORTRAN Program to Calculate Added Mass and Damping of Two-Dimensional Floating Bodies by the Boundary Element Method," DREA Technical Communication 90/302, March 1990.

22. M. Abramowitz and I.A. Stegun, *Handbook of Mathematical Functions*, Dover Publications, New York, 1965.

23. R.D. Cook, *Concepts and Applications of Finite Element Analysis*, John Wiley & Sons, New York, 1981.

24. C.J. Garrison and R.B. Berklite, "Impulsive Hydrodynamics of Submerged Rigid Bodies," *Journal of the Engineering Mechanics Division* **99**(EM1), 99–120 (1973).

25. C.J. Garrison, "Hydrodynamic Loading of Large Offshore Structures," in *Numerical Methods in Offshore Engineering*, edited by O.C. Zienkiewicz, O.C. Lewis, and K.G. Stagg (John Wiley & Sons, Chichester, England, 1978), pp. 87–139.

26. J.N. Newman, *Marine Hydrodynamics*, MIT Press, Cambridge, Massachusetts, 1977.

27. F. Ursell, "On the Rolling Motion of Cylinders in the Surface of a Fluid," *Quarterly Journal of Mechanics and Applied Mathematics* **II**(3), 335–353 (1949).

28. T. Dickinson and K. McTaggart, "Validation of Wave Excitation Force Prediction for the Submarine Motion Code SUBMO2," DREA Technical Communication 94/208, May 1994.

29. W.D. Kim, "On a Free-Floating Ship in Waves," *Journal of Ship Research* pp. 182–191,200 (1966).

UNCLASSIFIED

SECURITY CLASSIFICATION OF FORM
(highest classification of Title, Abstract, Keywords)

DOCUMENT CONTROL DATA

(Security classification of title, body of abstract and indexing annotation must be entered when the overall document is classified)

1. ORIGINATOR (The name and address of the organization preparing the document. Organizations for whom the document was prepared, e.g. Establishment sponsoring a contractor's report, or tasking agency, are entered in section 8.)

Defence Research Establishment Atlantic
P.O. Box 1012, Dartmouth, N.S. B2Y 3Z7

2. SECURITY CLASSIFICATION (overall security of the document including special warning terms if applicable.)

UNCLASSIFIED

3. TITLE (The complete document title as indicated on the title page. Its classification should be indicated by the appropriate abbreviation (S,C.R or U) in parentheses after the title.)

Improved Boundary Element Methods for Predicting Sectional Hydrodynamic Coefficients for Strip Theory Ship Motion Progams

4. AUTHORS (Last name, first name, middle initial. If military, show rank, e.g. Doe, Maj. John E.)

McTaggart, Kevin A.

5. DATE OF PUBLICATION (Month and year of publication of document.)

March 1996

6a. NO. OF PAGES (Total containing information. Include Annexes, Appendices, etc.) 67

6b. NO. OF REFS. (Total cited in document.) 29

6. DESCRIPTIVE NOTES (The category of the document, e.g. technical report, technical note or memorandum. If appropriate, enter the type of report, e.g. interim, progress, summary, annual or final. Give the inclusive dates when a specific reporting period is covered.)

DREA Technical Memorandum

8. SPONSORING ACTIVITY (The name of the department project office or laboratory sponsoring the reseach and development. Include the address.)

Defence Research Establishment Atlantic
P.O. Box 1012, Dartmouth, N.S. B2Y 3Z7

9a. PROJECT OR GRANT NUMBER (If appropriate, the applicable research and development project or grant number under which the document was written. Please specify whether project or grant.)

Project 1.g.2

9b. CONTRACT NUMBER (If appropriate, the applicable number under which the document was written.)

10a. ORIGINATOR'S DOCUMENT NUMBER (The official document number by which the document is identified by the originating activity. This number mrst be unique to this document.)

DREA Technical Memorandum 96/212

10b. OTHER DOCUMENT NUMBERS (Any other numbers which may be assigned this document either by the originator or by the sponsor.)

11. DOCUMENT AVAILABILITY (Any limitations on further dissemination of the document, other than those imposed by security classification)

(X) Unlimited distribution
( ) Distribution limited to defence departments and defence contractors; further distribution only as approved
( ) Distribution limited to defence departments and Canadian defence contractors; further distribution only as approved
( ) Distribution limited to government departments and agencies; futher distribution only as approved
( ) Distribution limited to defence departments; further distribution only as approved
( ) Other (please specify):

12. DOCUMENT ANNOUNCEMENT (Any limitation to the bibliographic annoucement of this document. This will normally correspond to the Document Availability (11). However, where futher distribution (beyond the audience specified in 11) is possible, a wider announcement audience may be selected.)

Unlimited

UNCLASSIFIED

SECURITY CLASSIFICATION OF FORM

DCDO3 2/06/87

13. ABSTRACT (a brief and factual summary of the document. It may also appear elsewhere in the body of the document itself. It is highly desirable that the abstract of classified documents be unclassified. Each paragraph of the abstract shall begin with an indication of the security classification of the information in the paragraph (unless the document itself is unclassified) represented as (S), (C), (R), or (U). It is not necessary to include here abstracts in both official languages unless the text is bilingual).

This technical memorandum presents two improved boundary element methods for predicting hydrodynamic coefficients of two dimensional sections. The first method is a source distribution method, while the second is a direct method for determining velocity potential. A major objective of these improved methods is to eliminate errors due to irregular frequencies, which currently exist in the close-fit method used by the strip theory program SHIPMO. Both new methods successfully eliminate problems caused by horizontal and vertical line segments with the close-fit method. To eliminate irregular frequencies of surface-piercing sections, the source distribution method employs additional sources on a deck lid at the waterline. The introduction of a deck lid eliminates some irregular frequencies but introduces new irregular frequencies. Alternatively, a modified direct method effectively eliminates all irregular frequencies. Future strip theory implementations should incorporate this modified direct method. This technical memorandum also reviews low and high frequency limits of hydrodynamic coefficients.

14. KEYWORDS, DESCRIPTORS or IDENTIFIERS (technically meaningful terms or short phrases that characterize a document and could be helpful in cataloguing the document. They should be selected so that no security classification is required. Identifiers, such as equipment model designation, trade name, military project code name, geographic location may also be included. If possible keywords should be selected from a published thesaurus. e.g. Thesaurus of Engineering and Scientific Terms (TEST) and that thesaurus-identified. If it not possible to select indexing terms which are Unclassified, the classification of each should be indicated as with the title).

added mass
damping
hydrodynamic coefficients
strip theory
boundary integral method